REPORT DOCUMENTATION PAGE

Form Approved OMB No. 0704-0188

1. REPORT DATE *(DD-MM-YYYY)*	2. REPORT TYPE	3. DATES COVERED *(From – To)*
15-07-2010	Final Report	01-Jan-07 - 15-Jul-10

4. TITLE AND SUBTITLE

Computer modeling of the physico-chemical processes for directed solidified ceramic composites of LaB6-MeB2 (Me-Ti, Zr, Hf) at macro-, meso- and microstructure levels

5a. CONTRACT NUMBER
STCU Registration No: P-273

5b. GRANT NUMBER

5c. PROGRAM ELEMENT NUMBER

6. AUTHOR(S)

Dr. Valeriy V Kartuzov

5d. PROJECT NUMBER

5d. TASK NUMBER

5e. WORK UNIT NUMBER

7. PERFORMING ORGANIZATION NAME(S) AND ADDRESS(ES)
I.M. Frantsevich Institute for Problems of Materials Sciences NAS of Ukraine
3 Krzhyzhanovsky str.
Kyiv 03680
Ukraine

8. PERFORMING ORGANIZATION REPORT NUMBER

N/A

9. SPONSORING/MONITORING AGENCY NAME(S) AND ADDRESS(ES)

EOARD
Unit 4515 BOX 14
APO AE 09421

10. SPONSOR/MONITOR'S ACRONYM(S)

11. SPONSOR/MONITOR'S REPORT NUMBER(S)
STCU 06-8009

12. DISTRIBUTION/AVAILABILITY STATEMENT

Approved for public release; distribution is unlimited.

13. SUPPLEMENTARY NOTES

14. ABSTRACT

This report results from a contract tasking I.M. Frantsevich Institute for Problems of Materials Sciences NAS of Ukraine as follows: Employing the methods of computer modeling, this effort is to investigate regularities of formation of microstructure of ceramic in-situ composites with the purpose of optimization of their physical and chemical properties and appropriate service characteristics. The object of this investigation is eutectic boron-boride composites (a model system is LaB6 - MeB2 (Me-Ti, Zr, Hf)). The tasks of this investigation are to define regularities of crystal-orientation ratios in conditions of eutectic co-crystallization of specified composites (that provides knowledge about a nature of formation of interfaces at directed solidification) and to model fracture processes of the investigated composites at chosen schemes of loading. Computer modeling shall be performed on the base of experimental data provided by IPMS colleagues (Dr. W. Paderno's REE Refractory Compounds Laboratory) and Dr. Ali Sayir at Case Western Reserve University (CWRU).

15. SUBJECT TERMS
EOARD, Materials, Ceramics Refractories and Glass

16. SECURITY CLASSIFICATION OF:			17. LIMITATION OF ABSTRACT	18, NUMBER OF PAGES	19a. NAME OF RESPONSIBLE PERSON
a. REPORT	b. ABSTRACT	c. THIS PAGE			WYNN SANDERS, Maj, USAF
UNCLAS	UNCLAS	UNCLAS	UL	79	19b. TELEPHONE NUMBER *(Include area code)* +44 (0)1895 616 007

P-273 (EOARD 068009)

COMPUTER MODELING OF BASIC PHYSICO-CHEMICAL PROCESSES FOR DSEC COMPOSITES OF SYSTEM LAB_6- MEB_2(ME-TI, ZR, HF) AT MACRO-, MESO- AND MICROSTRUCTURE SCALES

Final report

Kyiv, 2010

CONTENT

List of figures

List of tables

List of Symbols, Abbreviations, and Acronyms

T_0 – initial temperature of process;

T_c - temperature of crystallization;

c_0 - concentration of fibers MeB_2 (component B);

v - composite's pulling rate;

ρ - melt's density;

c_l , C_p – specific heat capacity of melt;

q - specific melting heat;

λ - coefficient of heat conductivity of melt;

γ - surface energy of interface LaB_6-MeB_2;

a - temperature conductivity;

$V_{кр}$ – substance volume in crystal state;

$V_{ж}$ – substance volume in liquid state;

$\sigma_{ГР}$ - critical stress for crack development under loading at plane stressed state;

c – crack's length;

E – Young's modulus;

K_{1C} – fracture toughness coefficient of material;

A, B - composite components, insoluble in each other, A - matrix, B - fibers;

ε - thickness of crystallization front;

N - number of fibers per unit of cross section,

W - heat flow, spent on composite's crystallization and fibers formation;

$c_1 = 1 - c$ - concentration of component A;

$\vec{v}_A$ - velocity of diffusion flow of component A;

$\vec{v}_B$ - velocity of diffusion flow of component B;

D, D^T - coefficients of mass-diffusion and thermo-diffusion respectively;

$T_1(x,t), \quad T_2(x,t)$ - temperatures distribution;

T^* - given ultimate temperature;

Ω - area correspondent to sample of investigated material;

$\mathcal{V}$ – Poisson's ration;

x_{mass} – mass share, MeB_2;

ρ_g / ρ_m - ratio of inclusion density to matrix density;

c_{vol} – volume share MeB_2;

α_g / α_m – ratio of coefficients of volume expansion of matrix and inclusion;

C_{ij} – composites' effective modules of elasticity;

SPM – scanning probe microscopy;

F - free energy;

U - internal energy;

S - system’s entropy;

SU – structural units;

ED – electron density;

Acknowledgement

Authors herewith would like to acknowledge Joan Fuller (AFOSR) and Dr. Ali Sayir (NASA Glenn) for initial impetus, ideas and fruitful discussion of the obtained results as well as AFOSR and EOARD for financial support of partner STCU project P273.

Introduction

The objective of this work was declared as «Investigation of regularities of formation of microstructure of ceramic *in-situ* composites by the methods of computer modeling with the aim to optimize their physico-chemical properties and correspondent service characteristics». This final report is to illustrate how we achieved the above said goal. Let's emphasize that this objective should be considered with two essential limitations. The first comes from a title of the project – this work considered only DSEC for systems LaB_6 – MeB_2 (Me-Ti, Zr, Hf) and basic physico-chemical processes (i.e. at this stage the composites are considered not as a material for final products but as a material - sample, material-prototype) were investigated for those systems. The second one falls from Proposal wording that this work is completely a pioneer one. That is why the work carried out should be considered as only the first steps towards the above said objective but not as accomplished research.

Conceptual part of this report mainly presents the results obtained by project team followed by our comments about similar problems highlighted in literature and formulate problems needed to be solved in the near future to achieve the above said "big" declared objective. During three years our team worked out more than 20 monographs and 400 papers with key words «directed solidification, eutectics, boride-boride composites, computer modeling». Participation in the workshops on directed crystallization held in Cleveland (USA), Kyoto (Japan), Saint Luis (USA), Seville (Spain), as well as materials science international conferences hosting correspondent sections enabled us a possibility to collect the information providing a rather complete understanding of this problem in the world and the results obtained. We are not going to list all references but only those needed for this report.

First of all we would like to remind that the objects of our investigation are boride-boride composites of the systems LaB_6 – MeB_2 (Me-Ti, Zr, Hf) obtained by the technology of directed solidification. In the Proposal we indicated that directed solidified «in-situ» composites with ceramic matrix were developed in Frantsevich Institute for Problems in Materials Science NAS of Ukraine [1]-[8]. 1982 year can be considered as a reference point for production of the first samples and the first paper [1] was published in 1983. English version of this paper came to light in 1990 [2]. In this work we would not raise a question of priority the above is only to highlight a solid scientific contacts with a technical laboratory highly experienced in growing of investigated composites. For a long time this laboratory had been headed by Dr. Yu. B. Paderno. Now, Dr. V.Filipov, his PhD student, who supervises a parallel project P276, heads it and our teams work together hand by hand.

The investigations were carried out at macro-, meso and micro scales and each scale is considered in own section.

1. Experiment

Currently the investigation of peculiarities of processes and growing of single crystals of borides of rare earth metals is performed by a few labs of the world - Japan, USA, Germany, Russia, Ukraine, and the methods of zone melting is used only in IPMS NASU and some labs of Japan. A number of

laboratories involved in experimental investigations of physical properties of these materials, is constantly growing all over the world, and all of those are interested in samples required for their research.

The Laboratory of Refractory Compounds of IPMS NASU (Dr. V.B. Filipov) is a vanguard from this stand point, the technologies of growth of boride single crystals with coherent character of melting developed in this lab are rather competitive and in some cases are better than those available in other countries [9, 10].

Samples produced in this laboratory are widely investigated in joint works with leading laboratories all over the world (USA, France, Germany, Poland, Slovakia, Israel, Russia, Switzerland, Italy, etc.).

In the Laboratory a process of directed solidification was carried out on special device «Crystal-111» for zone melting of refractory compounds, which was designed in Saint Petersburg according to IPMS technical assignment.

A speed of rods movement and rotation makes 18 mm/min and 30 rot/min respectively. The installation (see fig. 1.1) provided an opportunity of investigation of the process of directed solidification of a wide class of composite materials and to develop optimum technological parameters of the process. Arc melting was carried out by means of standard arc furnaces.

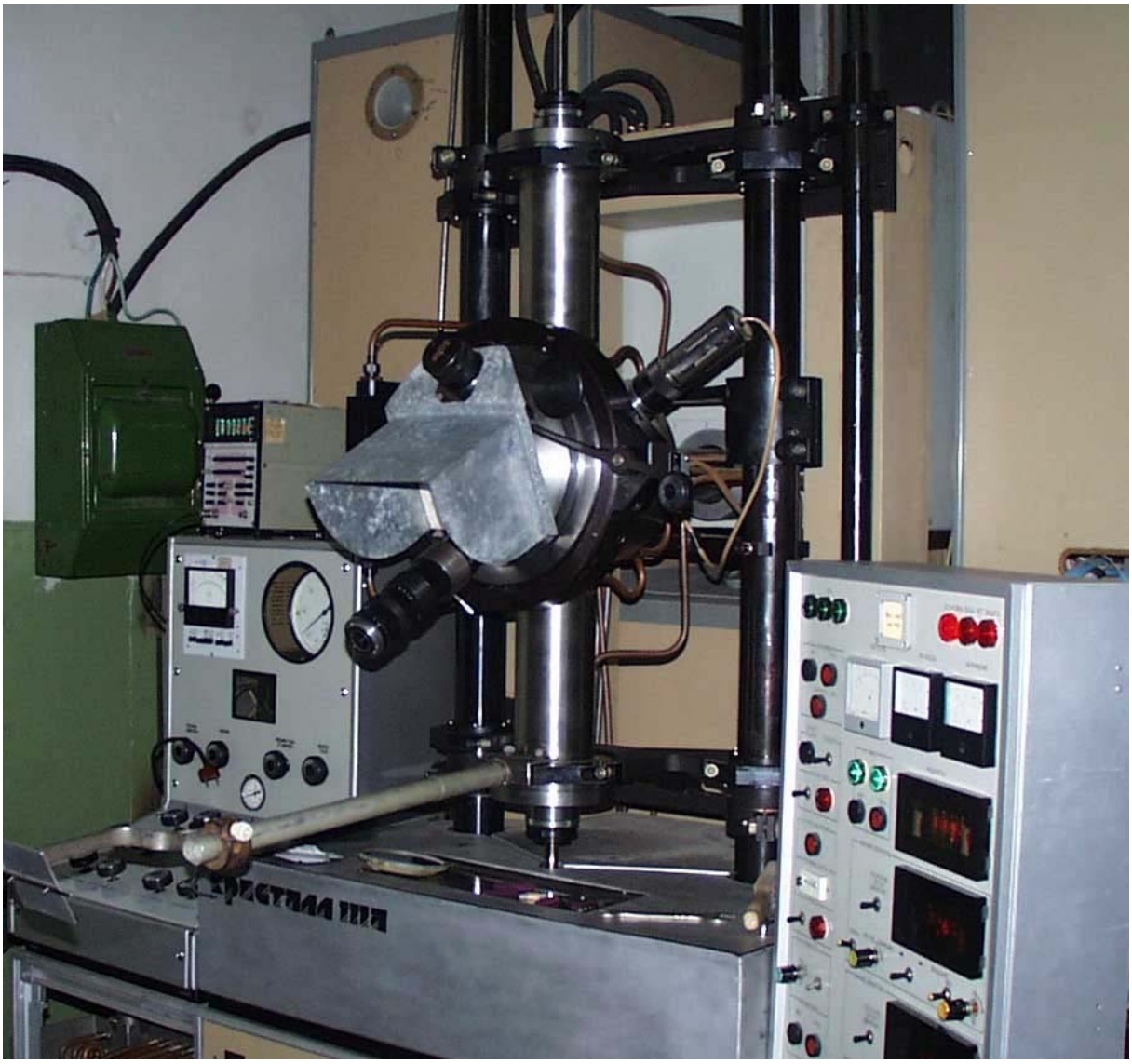

Fig 1.1 – General view of modernized installation „Crystal 111”, designed for zone melting of refractory compounds

Thus experimental data of our research are based on investigation of samples of directed solidified boride eutectics obtained according to a scheme below (see fig. 1.2).

DSEC

- Polycrystal feeding rod of eutectic composition

- Growth can be initiated on specifically oriented crystal

- Growth rates are usually found in a range 3-16 mm/min

- Variants of heating mechanism
- Focused irradiation
- Resistive heaters

- Controlled inert environment

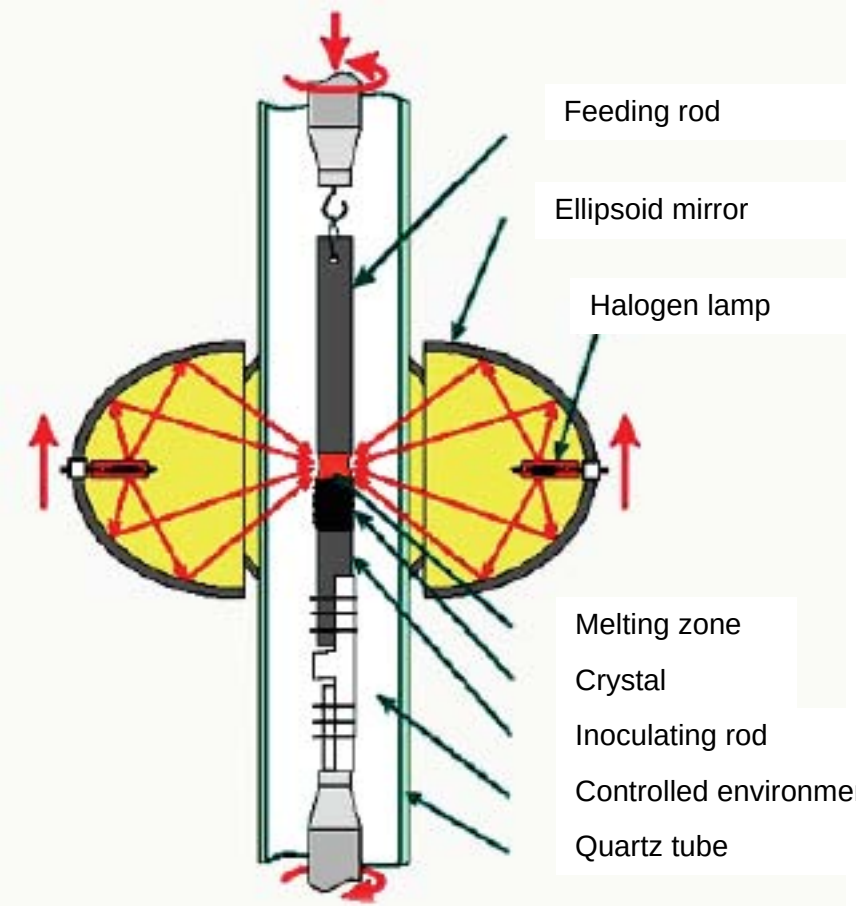

a) installation scheme

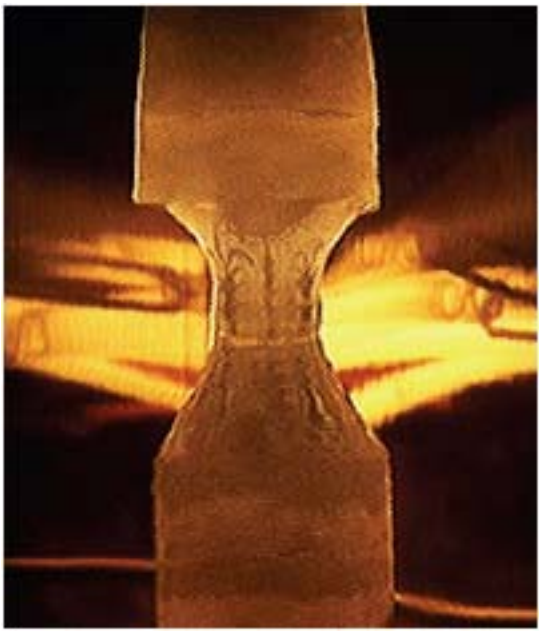

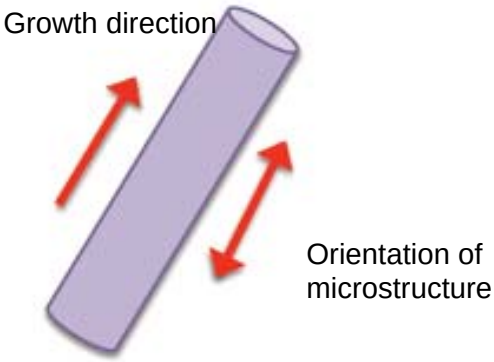

b) photo of melt zone

c) growth direction

Fig. 1.2. Scheme of production of samples of directed solidified boride-boride eutectics

Let's illustrate a number of electron microscope images of model samples of the investigated systems (see fig.1.3).

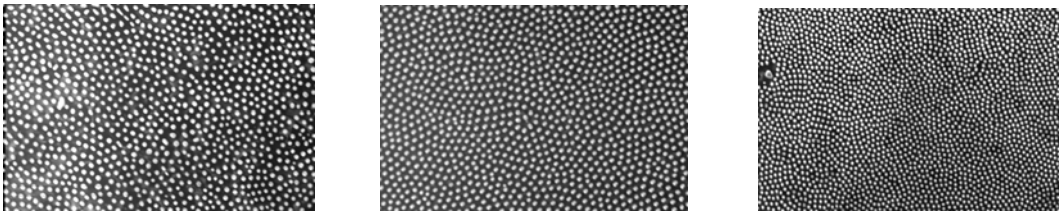

a) b) c)

Fig. 1.3 Dependence of structure of composite LaB_6-ZrB_2 vs crystallization rate mm/min: a – 3, b – 5, c - 10

It should be noted that a problem of reliable experimental data required for computer modeling at all (macro, meso and micro) structural scales was the biggest problem in this work.

Calculations at macro scale required the following data:

Definition of the main physical parameters

T_0 – initial temperature, K;

$T_1 < T_c$ in moving coordinates, T_c - temperature of crystallization K;

c_0 - concentration of fibers;

v - pulling rate of composite, m/sec;

ρ - density of melt, kg/m^3;

c_l - specific heat capacity of melt, Joule/kg K;

q - specific heat of melting, Joule/kg;

λ - coefficient of melt heat conductivity, Wt/m K or Joule/sec m K;

γ - surface energy of interface $A-B$, Joule/m^2;

a - temperature conductivity, m^2/sec.

Data interval for LaB_6-ZrB_2

1. CONCENTRATION

According to [11] compositions of alloys and melting temperature for *LaB_6-MeB_2* are available in Table 1.1:

Table 1.1 Alloys compositions and melting temperatures of eutectic alloys *LaB_6-MeB_2*

Boride phase	$T_{melting}$, K	% MeB_2 in eutectic		
		Mass	Vol.	Mol
TiB_2	3250	15*	16	34
ZrB_2	3310	20	16	32
HfB_2	3620	30	16	30

2. VELOCITY

According to Dr. Filipov's data a velocity of eutectic solidification for the system *LaB_6-ZrB_2* makes V=(0-0,833)*10^{-4} m/sec or V=0-5 mm/min.

3. MELT DENSITY

At room temperature from [11]

ρ *TiB_2* = 4 520 kg/m^3

ρ *ZrB_2* =6 090 kg/m^3

ρ *HfB_2* =11 200 kg/m^3

ρ *LaB_6* =4 730 kg/m^3

Let's define melt's density using the following ratio:

$$\rho_{ж} = \frac{V_{кр}}{V_{ж}} \rho_{кр}$$

$V_{кр}$ – substance volume in crystal state;

$V_{ж}$ – substance volume in liquid state;

Dr. Filipov reports that a shrinkage hole of solidified sample makes approx. 10%.

4. HEAT CONDUCTION

At room temperature from [11]

λ TiB_2 = 64,5 Wt/m К

λ ZrB_2 = 58,2 Wt/m К

λ HfB_2 = 51,1 Wt/m К

λ LaB_6 = 47,7 Wt/m К

We calculate a heat conduction using a rule of mixtures for LaB_6-MeB_2

5. SPECIFIC HEAT CAPACITY

At room temperature from [11]

c_l TiB_2 = 636 Joule/kg К

c_l ZrB_2 = 445 Joule/kg К

c_l HfB_2 = 249 Joule/kg К

c_l LaB_6 = 572 Joule/kg К

We calculate a specific heat capacity using a rule of mixtures for composite

6. SURFACE ENERGY

For calculations we used characteristics of mechanical properties of eutectic alloys LaB_6 - MeB_2, available in table 1.2.

Table 1.2 Characteristics of mechanical properties of eutectic alloys LaB_6 - MeB_2

Material	Bending Strength $\sigma_{изг}$, MPa	Fracture toughness) K_{1C}, MPa·m$^{1/2}$
LaB_6 - ZrB_2	1000...1320	15,2…18,3
LaB_6 - HfB_2	1150...1250	11,0...14,4
LaB_6 - TiB_2	388...656	15,2...16,5

From Griffith criteria we define a surface energy [13]:

$$\sigma_{ГР} = \sqrt{\frac{2\gamma E}{\pi c}} \qquad (1.1)$$

where

$\sigma_{ГР}$ - critical stress for crack development under load at plane stressed state;

c – crack's length;

E – Young's modulus;

γ - surface energy.

$\sigma_{ГР}$ is found out from a ratio to define fracture toughness K_{1C}, namely: $K_{1C} = \sigma_{ГР}\sqrt{\pi c}$, where c – admissible crack's size .

$$\sigma_{TP} = \frac{K_{1C}}{\sqrt{\pi c}} \quad (1.2)$$

Substituting (2) into (1) we obtain an expression for surface energy:

$$\gamma = \frac{K_{1C}{}^2}{2E} \quad (1.3)$$

Young's modules values for the investigated alloys are borrowed from [14].

E(TiB$_2$) = 540, 53 GPa; *E(ZrB$_2$)* = 495, 8 GPa; *E(HfB$_2$)* = 479,71 GPa; *E(LaB$_6$)* = 478,73 GPa

Experimental values of Young's modulus along fiber (given by Dr. V. Filipov) for *LaB$_6$-ZrB$_2$* = 420 GPa.

By formula (1.3):

$\gamma = \frac{12^2}{2 \cdot 420} = 0{,}170 \frac{10^{12}}{10^9}$ Pa= 170 Joule/m^2

8. SPECIFIC HEAT OF MELTING

For borides there are neither experimental nor reference data.

According to [13] specific heat of melting for solid bodies in found in interval (24,7 – 266) KJoule/kg.

To investigate structure of fracture surface and microstructure of interfaces «fiber-matrix» required a package of images (obtained by scanning electron microscopy of rather high resolution) for the problems highlighted in the working schedule. However, unfortunately, these images were not submitted by project coordinator and thus the developed methodology of processing of electron-microscopy images by the methods of fractal geometry were tested and «adjusted» on images, which were borrowed from existing publications and those, which were kindly presented by our colleagues from IPMS NASU (but it were another objects).

The most favorable situation with experimental data was at microscale modeling. Here the required atomic constants and structure of the investigated systems are available in crystallographic literature.

It should be noted that issues of correctness of initial data for numerical experiment had been constantly discussed with Dr. Ali Sayir, scientific coordinator of this project (NASA Glenn Center, the USA). At present he developed a scheme of joint works of laboratories participating in "Big International Project" (the USA, France, Ukraine) to obtain experimental data required to proceed with computer modeling of the above said problems.

2. MACROSCALE. MODELING OF TECHNOLOGICAL PROCESS OF DIRECTED SOLIDIFICATION OF COMPOSITES OF EUTECTIC SYSTEMS LAB_6-MEB_2

At growth of single crystals from melt thermal conditions essentially influence on processes of crystals growth and quality. These conditions, first of all, are defined by crystals form and sizes, character and intensity of heat removal from external surfaces of a crystal, character and intensity of heat exchange in melt, velocity of elongation and heat-physical properties of solid and liquid phases. At crystallization

from multicomponent systems thermal conditions are also affected by diffusion processes in melt and change of temperature on interface depending on components concentration.

Thermal conditions, in their turn, define a form of crystallization front, growth rate and temperature gradients on interfaces as well as thermal stresses in crystals during growth. Knowledge of these parameters is required for production of perfect single crystals, both in macro- and micro-scales.

Now to obtain single crystals from melt different methods of directed solidification are employed [15,16]. The most known methods are the methods of Kiropulosa [17] and Tchohralsky [18] where crystallization occurs from top to down, and the methods of Stokbarger [19] and Shtobera [20] where it is carried out from below upwards. In all these methods heat removal is made, mainly, through the hardened crystal and a temperature field in a crystal has, as it is possible to believe, axial symmetry. Thus the front of crystallization is not always plane, and represents, in macroscopic scales, a surface of rotation from a variable on radius the curvature changing in due course. Usually distinguish the plane, convex and concave form of front of crystallization though in practice of cultivation of single crystals there can be found rather difficult cases.

As it is found out [21,22], the most favorable for a growth of single crystals is a plane and convex form of crystallization front whereas at concave front an origin of parasitic germs on a lateral surface of a crystal is quite possible and an opportunity of thinning of boundaries between twins or blocks with big angular disorientation that promotes polycrystal growth is absent.

On the other hand, the existence of plane front of crystallization at all stages of growth is associated with uniform heat removal from a crystal on its face surface, uniform heat exchange in melt on front of crystallization and absence of a lateral heat removal whereas a presence of appreciable lateral heat-removal aspires to give to crystallization front a concave form. Therefore the analysis of influence of thermal conditions on the form of crystallization front represents, undoubtedly a big interest.

The problem of definition of a law of promotion of crystallization front in temperature fields associated with it now is solved only for bodies of elementary form [23]: semi-planes [24,25], spheres [26], cylinder [27,28], paraboloid of revolution [29] and ellipsoid of revolution [30]. For fibrous composites being an object of investigation of this work as far as a literature review showed this problem has not been put as of yet. Therefore the problem of modeling of promotion of crystallization front in technology of directed crystallization of composites of systems LaB6-MeB2 (Me-Ti, Zr, Hf) is new and actual. The specific target, which attracts our interest, first of all, is to define a functional dependence of diameter of inclusion fiber (MeB2) vs. velocity of elongation of a firm phase of a composite. This is the most interesting for colleagues - technologists and it would be a priority for a macro-scale.

The composites of type LaB_6-MeB_2 are considered.

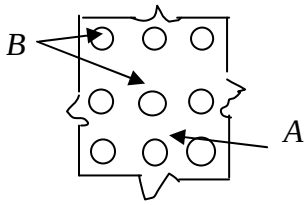

Fig.2.1 Scheme of fibrous composite.

Notations: A, B - composite components insolvent in each other. A - matrix (for instance, LaB_6), B - fibers. (MeB_2) d - fiber diameter; c_0 - concentration of component B

Let's write down approx integral laws of mass and energy conservation in cubic unit of two component composite at crystallization front $x = \delta$

$$\begin{cases} N\dfrac{\pi d^2}{4} = c_0 - substance\ conservation, \\ N\pi d\gamma v + qv = W \quad - energy\ conservation \end{cases} \tag{2.1}$$

where γ - surface energy of boundary $A-B$, q - specific heat of melting, N - number of fibers per volume unit, W - heat flow spent on crystallization and fibers formation.

From (2.1) falls a simple expression for composite fiber diameter

$$d = \frac{4\gamma c_0 v}{W - qv} \tag{2.2}$$

and a problem is to define a heat flow W, depending on temperature distribution T.

Fig. 2.2 illustrates a scheme of temperature distribution T in melt and fibrous composite at stable mode of formation of fibers with crystallization rate $v = const$ towards axis x.

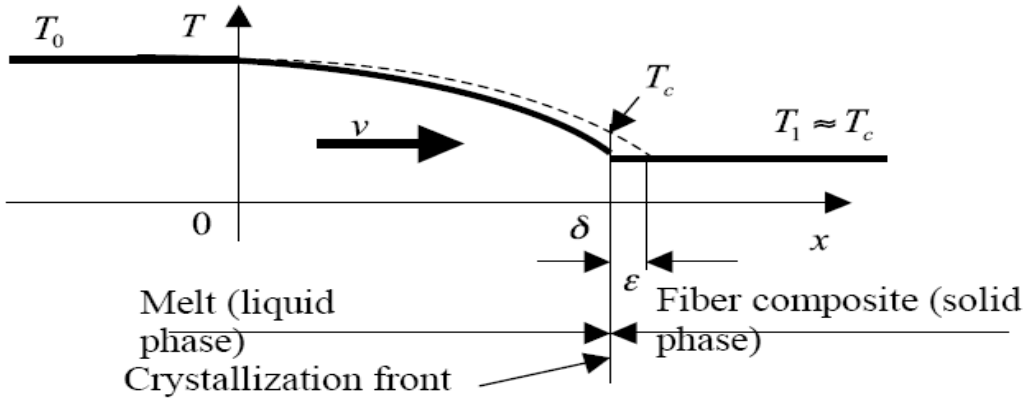

Fig.2.2 Scheme of distribution of temperature at stable mode $T_1 < T_c$ in moving coordinates. T_c - temperature of solidification, ε - thickness of crystallization front, $\dfrac{\varepsilon}{\delta} << 1$, v - velocity of composite elongation, $\dot{\delta}(t) = 0$.

On practice, the conditions of fibers growth on billet's axis and its periphery essentially differ. For modeling conditions of crystallization on billet's axis were considered. At this a rather grounded is a proposition that lateral (perpendicular to axis x) heat removal is absent. Its presence, in areas close to billet surface, makes inhomogeneity of composite in cross direction (along crystallization front). In

accepted model a heat flow is headed on axis x and is defined by temperature distribution along this axis (see fig.2.2).

This distribution obeys the equation of heat conductivity

$$\rho c_l \frac{\partial T}{\partial t} = \lambda \frac{\partial^2 T}{\partial x^2} - \rho c_l v \frac{\partial T}{\partial x}, 0 \le x \le \delta, t \ge 0,$$

where ρ - melt density, c_l - specific heat capacity of melt, λ - coefficient of melt's heat conductivity.

At stable mode temperature T depends on space coordinate x and is not time dependent. Thus instead of the last we obtain

$$\lambda \frac{\partial^2 T}{\partial x^2} - \rho c_l v \frac{\partial T}{\partial x} = 0, 0 \le x \le \delta. \tag{2.3}$$

Boundary conditions for (3) are defined by equalities:

$$T(0) = T_0, \quad T(\delta) = T_1, \tag{2.4}$$

since it is supposed that $T(x) = T_0$ at $x \le 0$ and $T(x) = T_1$ at $x \ge \delta$ (see fig.2.2).

A solution of boundary problem (2.3),(2.4) would be a function

$$T = T_1 + \frac{T_0 - T_1}{1 - \exp\left(\frac{v}{a}\delta\right)}\left(\exp\left(\frac{v}{a}x\right) - \exp\left(\frac{v}{a}\delta\right)\right), \quad a = \frac{\lambda}{\rho c_l} \tag{2.5}$$

where a - temperature conductivity.

The first integral of equation (2.3) (mass conservation law) can be written as

$$\lambda \frac{\partial T}{\partial x} - \rho c_l v T = -\rho c_l v T_1 - W = const. \tag{2.6}$$

Here we suppose that: $\rho v = \rho_s v_s$ (flow's continuity), $c_l = c_s$, where index s is referred to composite solid phase.

From here and (2.5) for a value of heat flow W we obtain

$$W = \frac{T_0 - T_1}{\exp\left(\frac{v}{a}\delta\right) - 1} \rho c_l v \exp\left(\frac{v}{a}\delta\right). \tag{2.7}$$

Thus, from (2.2) and (2.7) to evaluate fiber diameter d we have

$$d = \frac{4\gamma c_0}{\rho c_l \left(T_0 - T_1\right) - q \exp\left(-\frac{v}{a}\delta\right)} \left(1 - \exp\left(-\frac{v}{a}\delta\right)\right). \tag{2.8}$$

If to introduce notations:

$\eta = \frac{v}{a}\delta, \quad \Delta(\eta) = 1 - \exp(-\eta)$,

then the main evaluative formulas for d and W can be written as:

$$d = \frac{4\gamma c_0 \Delta(\eta)}{\rho c_l \left(T_0 - T_1\right) - q\left(1 - \Delta(\eta)\right)}, \qquad W = \frac{\left(T_0 - T_1\right)\rho c_l v}{\Delta(\eta)} - qv. \tag{2.9}$$

Noteworthy A case $c_l \neq c_s$ is considered similarly. For this case we have

$$W = \frac{\rho v c_l}{1 - \exp(-\eta)} \left[T_0 - \frac{c_s}{c_l} T_1 + \left(1 - \frac{c_s}{c_l}\right) T_1 \exp(-\eta) \right], \tag{2.10}$$

$d = \frac{4\gamma c_0 v}{W - qv}$.

From (2.2), (2.9) and the last formula, we immediately obtain the following required (but not sufficient) conditions of fibers formation:

$$v > 0, \quad W > qv, \quad \rho c_l \left(T_0 - T_1\right) > q\left(1 - \Delta(\eta)\right). \tag{2.11}$$

To define a physical meaning of η, let's re-write it as follows:

$$\eta = \frac{v}{a}\delta = \frac{v\rho c_l \delta \left(T_0 - T_1\right)}{\lambda \left(T_0 - T_1\right)} = \frac{v\rho c_l \left(T_1 - T_0\right)}{\lambda \left\langle grad\ T \right\rangle} \quad , \tag{2.12}$$

where $\left\langle grad\ T \right\rangle$ - average value of temperature gradient on the part $(0; \delta)$.

From the above follows that value η is a ratio of convective heat flow (at the expense of extension of crystal with velocity *v*) to heat flow, caused by heat conductivity. Value η essentially depends on value δ, which definition requires to consider and investigate non-stationary mode of crystallization, i.e. solution of appropriate Stephan's problem, analysis of solution stability at variations of v and existence of stable modes of crystallization. Obviously value δ depends on velocity v and fiber diameter d. Thus in reality, the dependencies (2.9) and (2.10) are more complicated.

Analysis of simplified evaluative dependencies (2.9), (2.10) shows that

$$\lim_{v\to 0} d = 0,$$
$$\lim_{v\to\infty} d = d_{\max} = \frac{4\gamma c_0}{\rho c_l \left(T_0 - T_1\right)}. \qquad (2.13)$$

Fig 2.3 illustrates schematically functions (2.9), (2.10). Experiments show [31], that at rather high velocities $v > v_{\max}$ there occurs unstable formation of fibers, their break or they just have no time to form. At velocities $v < v_{\min}$ there is not uniform distribution of fibers, and fibers diameter fluctuates. That is why there exists the interval of velocities $\left(v_{\min} < v < v_{\max}\right)$, at which stable formation of composite homogeneous structure occurs and formulas (2.9), (2.10) (see fig.2.3) can be applied. Boundaries of this interval, obviously, may be defined and investigated by means of solution of Stephan's problem.

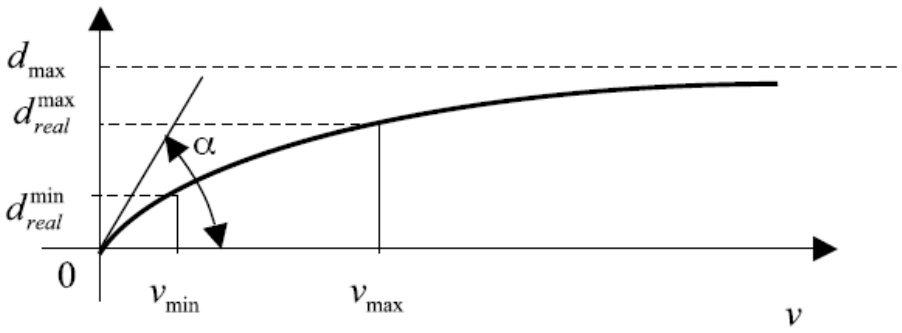

Fig. 2.3. Schematic dependence d vs v

As it follows from a comparison of the results of computing experiment with those of natural one a character of dependence coincides but not numerical characteristics. The reason of it one may to find out in discrepancies of performance f initial data and necessity of adjustment of the model itself. Therefore to achieve further progress in modeling of directed crystallization it is necessary to work on the problems outlined below.

TASK №1: To define a surface energy of crystallization front γ by the method of molecular dynamic

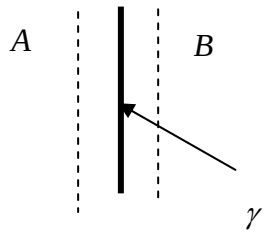

Fig. 2.4 Definition of surface energy of crystallization front γ

Approximate dependence γ vs. temperature T

$$\gamma(T) \approx \gamma(T_1) - \frac{\gamma(T_1) - \gamma(T_0)}{T_0 - T_1}(T - T_1)$$

Solution of the task 1 by the results of numerous discussions with materials science specialists from different countries and agreement with project coordinator is transferred to microstructural (atomic) scale and would be allocated as separate problem which would be investigated in the follow up project.

TASK №2: To define stationary distribution of concentrations C, C_1, of components A, B

Designations: c - concentration of component B, $c_1 = 1 - c$ - concentration of component A, $\vec{v}_A$ - velocity of diffusion flow of component A, $\vec{v}_B$ - velocity of diffusion flow of component B, D, D^T - coefficients of mass-diffusion and thermo-diffusion respectively, $\vec{v} = (v; 0; 0)$.

$$\vec{v}_A = \vec{v} - \frac{D}{c_1} grad\ c_1 - \frac{D^{T_A}}{Tc_1} grad\ T\ ,$$

$$\vec{v}_B = \vec{v} - \frac{D}{c} grad\ c - \frac{D^{T_B}}{Tc} grad\ T\ .$$

Inequality $\vec{v}_A \neq \vec{v}_B$ is obviously the main reason of corrugation of crystallization front.

By definition $\vec{\mathbf{v}} = c_1\vec{\mathbf{v}}_A + c\vec{\mathbf{v}}_B$, $1 = c + c_1$; from here and prior equalities we obtain

$$D^{T_A} + D^{T_B} = 0, \quad D^{T_B} = -D^{T_A} = D^T$$

Schematic representation of space area V (periodic cell), where equations of stationary diffusion are solved (see fig. 2.5).

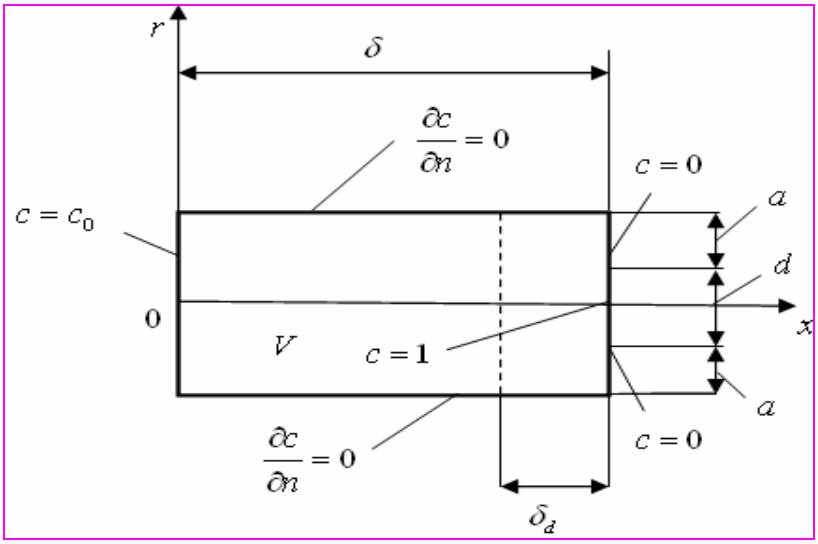

Fig. 2.5 Schematic illustration of space area V (periodic cell), where equations of stead state diffusion are being solved

Fig 2.5 also presents boundary conditions for $c(x,y,z)$, $c_0 \approx \dfrac{d^2}{(2a+d)^2}$ Equation of steady state diffusion to define $c(x,y,z)$

$$div\left[\rho\left(Dgrad\ c+\frac{D^{T_B}}{T}grad\ T\right)\right]-\rho v\frac{\partial c}{\partial x}=0,(x,y,z)\in V \qquad (13.2)$$

TASK №3 Definition of temperature distribution $T_1(x,t), T_2(x,t)$ and a low of movement of crystallization front $S(t)$ (non-stationary regime, Stephan's problem)

B. Non-stationary regime (Stephan's problem)

Crystallization front

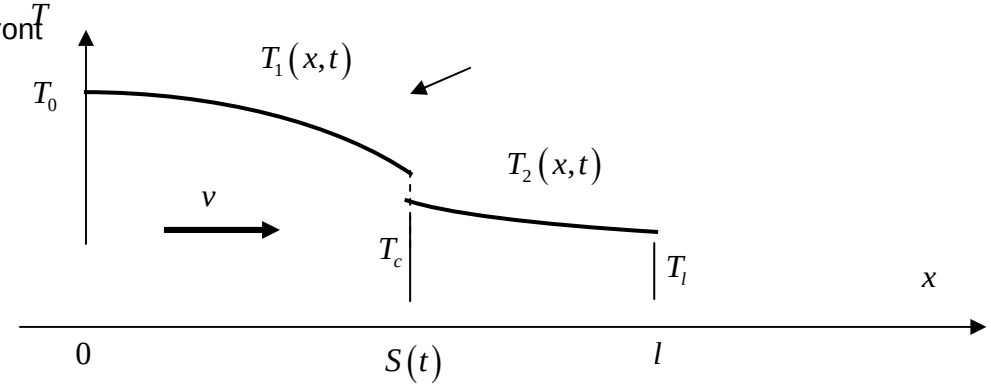

Fig. 2.6 Temperature distribution at non-stationary mode, $\frac{S}{l}<<1(l=\infty)$, $T_l<T_c$, $t\geq 0$.

Conditions of stationary mode

$$\lim_{t\to\infty}\delta(t)=\lim_{t\to\infty}\left(S(t)-vt\right)=\delta=const,$$

$$\lim_{t\to\infty}\dot{\delta}(t)=\lim_{t\to\infty}\left(\dot{S}(t)-v\right)=0.$$

Equations to define functions $T_1(x,t), T_2(x,t)$

$$\lambda\frac{\partial^2 T_1}{\partial x^2}-\rho c_p v\frac{\partial T_1}{\partial x}-\rho c_p\frac{\partial T_1}{\partial t}=0,\quad 0\le x\le S(t)$$

$$\lambda_s\frac{\partial^2 T_2}{\partial x^2}-\rho_s c_{ps} v\frac{\partial T_2}{\partial x}-\rho_s c_{ps}\frac{\partial T_2}{\partial t}=0,\quad S(t)\le x\le l$$

Boundary conditions

A) at the ends of $(0;l)$

$$T_1(0;t)=T_0,\ T_2(l;t)=T_l,\ t\ge 0$$

B) at crystallization front $S(t)$

$$T_1\left(S(t),t\right)=T_2\left(S(t),t\right)=T_c,\quad t\ge 0,$$

$$\lambda\left.\frac{\partial T_1}{\partial x}\right|_{x=S-0}-\lambda_s\left.\frac{\partial T_2}{\partial x}\right|_{x=S+0}=\sigma\dot{S}(t),\ \sigma=\frac{4\gamma c_0}{d}+q.$$

At limited temperature gradients from suppositions of model it falls an existence of upper ultimate velocity of stable crystallization $\dot{S}$

2.1. Definition of functional dependence of fiber diameter of inclusion (MeB_2) vs pulling rate of solid phase of composite

The conducted investigations showed that at low velocities of crystallization a deviation of dependence character of a number of fibers from crystallization velocity from linear dependence one is observed. At these crystallization rates even minimum deviation of composition from exact eutectic ratio brings to destabilization of a process of crucible free zone melting. Initially it was supposed that fixed deviations from generally accepted one inversely proportional to dependence of average fiber diameter of inclusion MeB_2 from crystallization velocity [32, 33] are caused by fluctuations of parameters of crystal growth. However after accumulation of experience in melting of these systems and additional justification of eutectic ratio of components we succeeded to stabilize the process of composite growth with low velocities of crystallization front. Dependencies of average diameter of fibers from crystallization rate in interval 0,5-12 mm/min were obtained. At crystallization velocities up to 4 mm/min, a number of fibers per unit of sample's cross section decreases with a growth of crystallization velocity i.e. their diameter grew

(see fig. 2.1.1). Thus the obtained results essentially differ from generally accepted representations [32, 33].

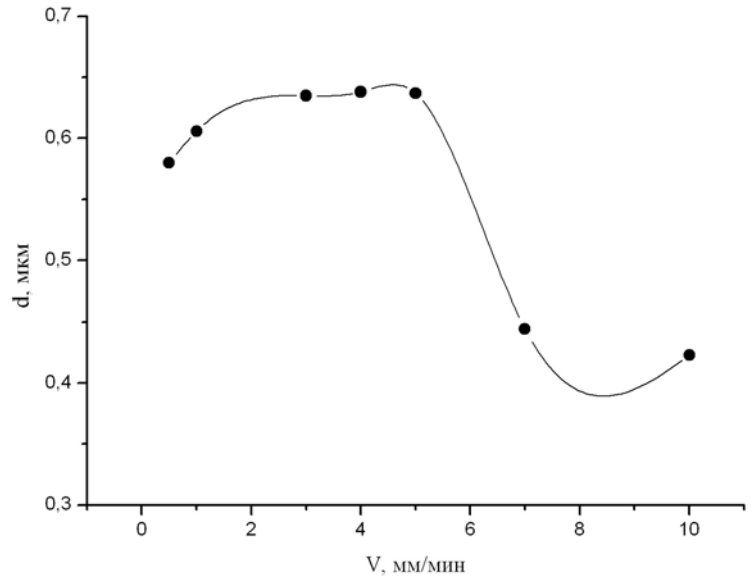

Fig. 2.1.1. Dependence of fiber diameter ZrB_2 (in system LaB_6-ZrB_2) vs crystallization rate (experimental data)

This result enabled to suppose that depending on given crystallization rate there exist a few mechanisms, which define size of structural elements of eutectic composites at their directed solidification.

On the base of model proposed in section 2 evaluative calculations for fiber diameter according to (2.9) were carried out. While calculating the authors faced a problem of absence of reliable information about a major part of experimental values of used physical parameters, what we had discussed in section 1.

Initial data of testing calculation of definition of dependence *d=f (v)* for the system LaB_6-ZrB_2:

c_0 =0,16; v =(0-0,833)10^{-4} m/sec; ρ = 4 498,20 kg/m^3; c_l = 827,52, Joule/kg K; q = 50*10^3 Joule/kg; ΔT = 100 K; λ = 74,07 Watt/m ; γ = 145 Joule/m^2

The results of carried out calculation are available on fig. 2.1.2.

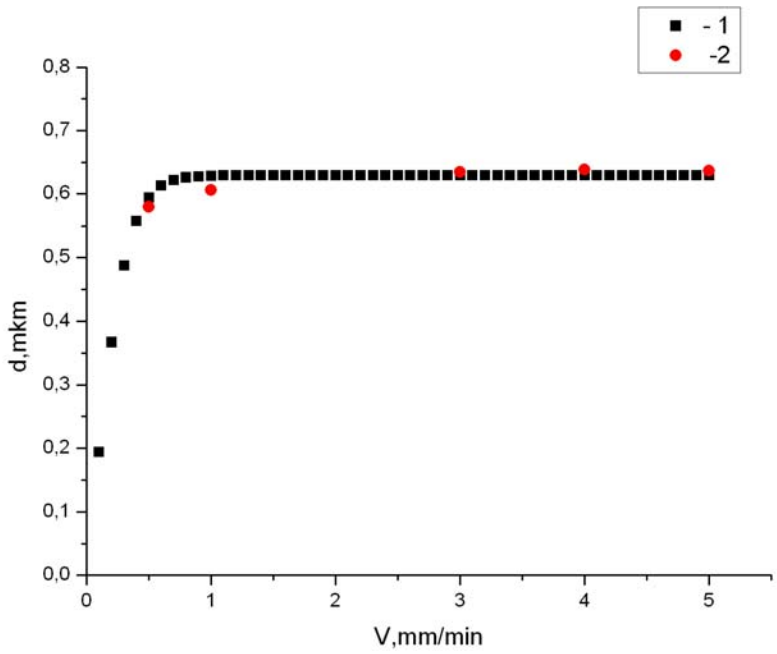

Fig.2.1.2. Dependence of fiber diameter vs pulling rate for LaB_6-ZrB_2:

1- calculated values;

2- experimental data

The simplest model of the process of directed solidification for boride composites MeB_6-MeB_2 is based on mass and energy conservation laws for a sample brings to a conclusion that in the mode of low velocities of crystallization 0,5 mm/min < v < 4 mm/min diameter of fiber of reinforcing component MeB_2 increases with a growth of crystallization rate, that points on a difference in crystallization mechanisms for the investigated materials depending on pulling rate.

To model crystallization processes of the investigated system in the whole technologically realized interval of pulling rate of solid phase component requires to consider more complicated mathematical models based on a solution on non-stationary Stephan's problem.

2.2 Steady state diffusion in binary eutectic systems at directed solidification from melt

Let's bring initial (ultimately simplified) solution of task 2 (see fig.2.5, equation 13.2)

Equation of steady state diffusion to define $c(x, y, z)$

Supposing $D = const, \quad D^T = const, \quad \rho = const$, we obtain

$$div\left(grad\ c + \frac{D^T}{TD} grad\ T \right) - \frac{v}{D}\frac{\partial c}{\partial x} = 0, \quad (x, y, z) \in V \tag{2.2.1}$$

From (12) falls, that at given T and boundary conditions, solution of this equation depends on two constants only: $\frac{D^T}{D}, \frac{v}{D}$. $\frac{D^T}{D}$ - thermo-diffusion solution.

If to neglect with thermo-diffusion then

$$divgrad\ c - \frac{v}{D}\frac{\partial c}{\partial x} = \Delta c - \frac{v}{D}\frac{\partial c}{\partial x} = 0, \quad (x, y, z) \in V \tag{2.2.2}$$

This equation can be reduced to Helmgotz's one

$$\Delta w + \kappa w = 0, \quad (x, y, z) \in V \quad , \tag{2.2.3}$$

where $\kappa = -\frac{v^2}{4D} < 0, \quad c = w\exp(\mu x), \quad \mu = \frac{v}{2D}$, Δ - Laplacian.

Knowing solution of equations (2.2.1)-(2.2.3) one may design velocity fields $\mathbf{v}_A, \mathbf{v}_B$ and current line

$$\frac{d\mathbf{x}_A}{ds_A} = \mathbf{v}_A, \quad \frac{d\mathbf{x}_B}{ds_B} = \mathbf{v}_B.$$

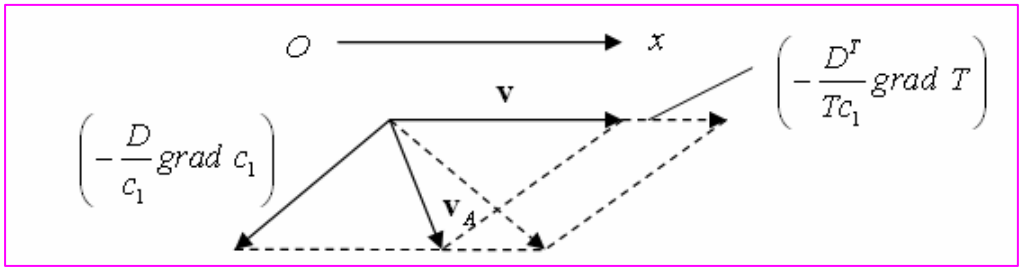

Fig. 2.2.1 Scheme of field velocity design

Numerical realization and results

Discrete analog to diffusion equation:

$$\frac{r_j + \frac{h}{2}}{r_j h^2}\left(c_{i,j+1} - c_{i,j}\right) - \frac{r_j - \frac{h}{2}}{r_j}\left(c_{i,j} - c_{i,j-1}\right) +$$
$$+ \frac{c_{i-1,j} - 2c_{i,j} + c_{i+1,j}}{h^2} - \frac{V}{D}\frac{c_{i+1,j} - c_{i-1,j}}{2h} = 0$$

$1 \prec i \prec n$

$1 \prec j \prec m$

when *i*=1:

$c_{i-1,j} = c_0$.

At *i=n:*

$$c_{i+1,j} = \begin{cases} 1, для\ точки\ j, которая\ расположена\ на\ волокне \\ 0, для\ точки\ j, которая\ расположена\ вне\ волокна \end{cases}$$

At *j*=1 point is on the axis of chosen cylinder. Thus instead of $\frac{1}{r}\frac{\partial}{\partial r}\left(r\frac{\partial c}{\partial z}\right)$ we have $\frac{\partial^2 c}{\partial r^2}$.

Apart from that the axis symmetry takes place, thus we use a condition: $c_{i0} = c_{i2}$.

At *j=m* $\frac{\partial c}{\partial r} = 0$ is true, for our case $\frac{c_{i,m+1} - c_{i,m}}{h} = 0$.

Initial data for numerical experiment:

d , fiber diameter = 0,6 mkm;

V, pulling rate = 0,5 m/sec;

a = 0.45 mkm

D, diffusion coefficient =0.00012 mm^2/sec

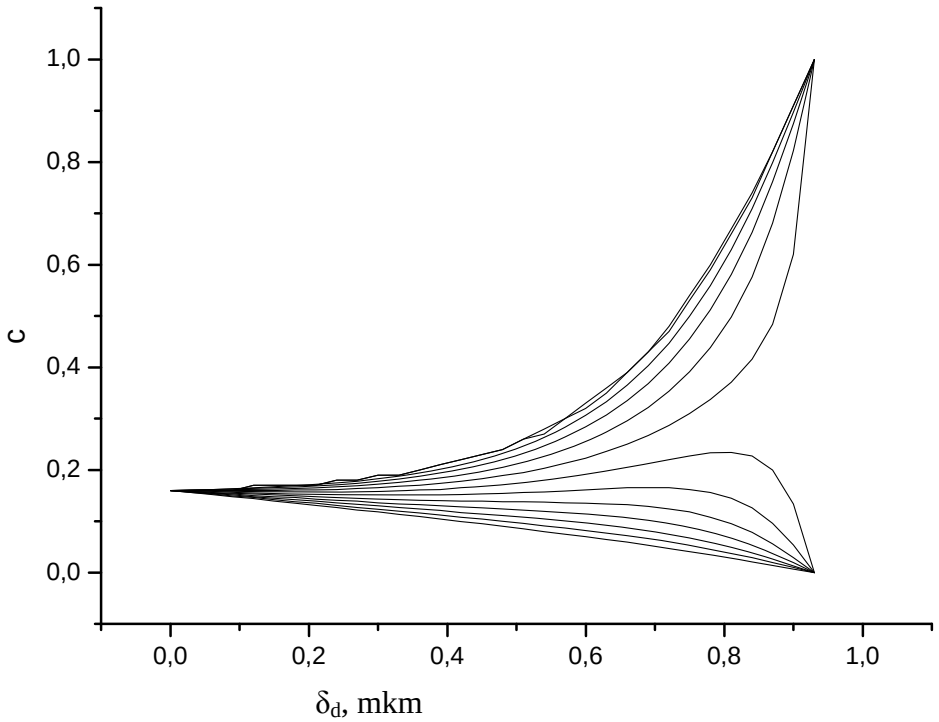

Fig. 2.2.2 Distribution of concentration *c* for component MeB_2 in the area of intensive diffusion δ_d

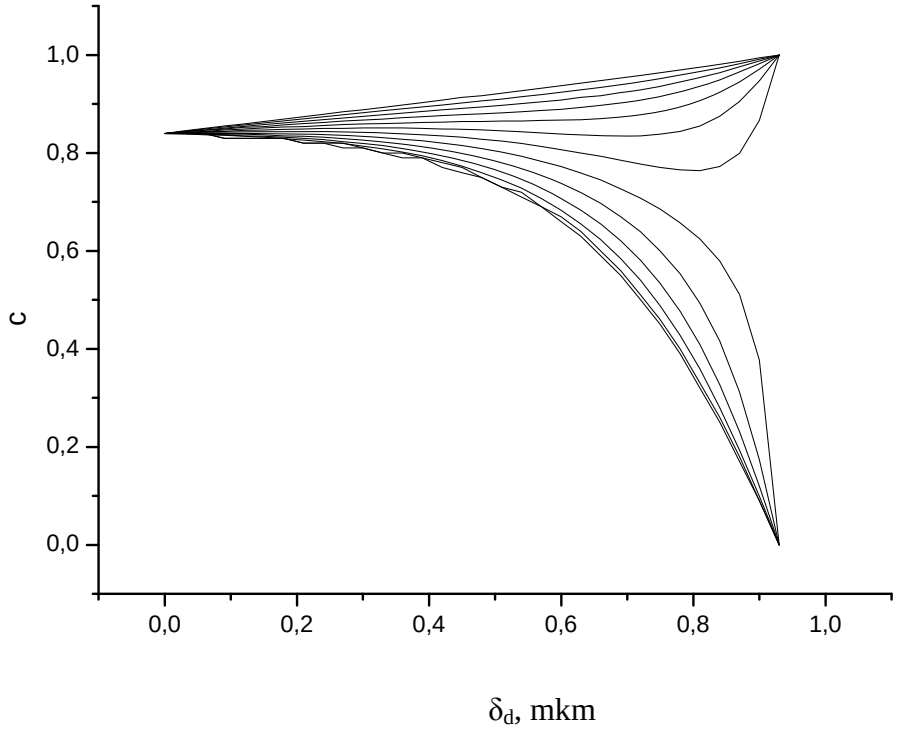

Fig.2.2.3 Distribution of concentration ***c*** for component LaB_6 in the area of intensive diffusion $\boldsymbol{\delta_d}$.

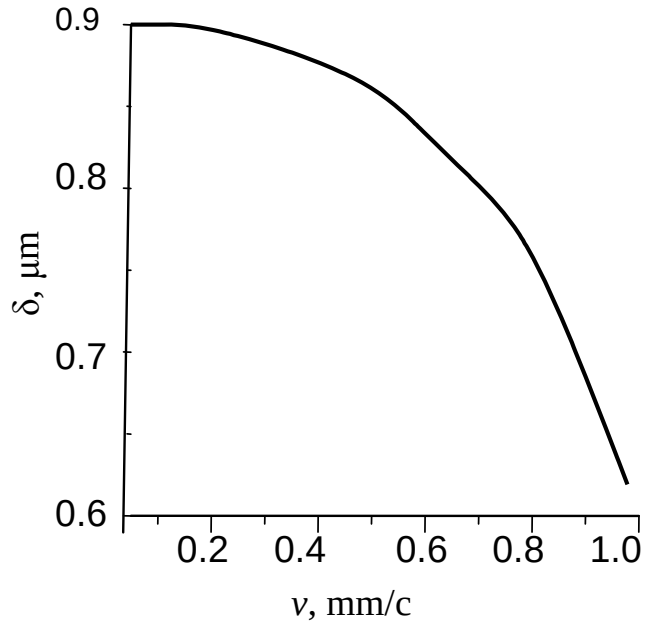

Fig. 2.2.4 Dependence of intensive diffusion zone size δd vs pulling rate *v*

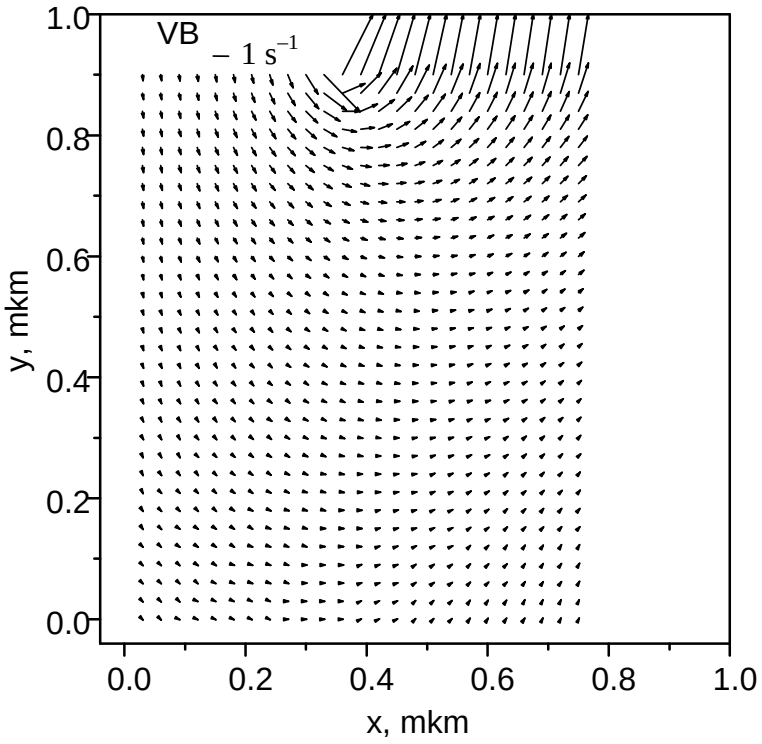

Fig. 2.2.5. Velocity fields for component ZrB_2

2.3. Solution of a problem of heat transfer with moving boundary caused by a change of substance aggregate state (Stephan's problem)

Task 3 was subjected to initial investigation. This problem of heat transfer with migrating boundary caused by change of aggregate state of substance is a problem of Stephan's type [34-41]. This class of problems is referred to one of the most difficult problems of mathematical physics. Classic variant of Stephan's problem is formulated for phase transitions like melting–crystallization, is reduced to equation of heat conductivity in the area with preliminary known interface dividing solid and liquid phase and having a temperature equal to temperature of phase transformation. Non-linearity of problem is governed by a presence of moving interface.

There are a small number of analytical solutions of similar problems, limiting by simplest cases. The most developed methods are numerical methods mostly contributed and developed in different time by A.A. Samarsky [42], B.M. Budak [34,35], P.N. Vabishevich [36].

We would be based on the method of potential [43]. Let's define temperature distribution $T_1(x,t), \quad T_2(x,t)$.

It is required to define function $T_1(x,t)$, $T_2(x, t)$ from equation

$$\frac{\partial^2 T_1}{\partial x^2} + q_1 \frac{\partial T_1}{\partial x} - p_1 \frac{\partial T_1}{\partial t} = 0, \quad 0 \le x \le S(t),$$
$$\frac{\partial^2 T_2}{\partial x^2} + q_2 \frac{\partial T_2}{\partial x} - p_2 \frac{\partial T_1}{\partial t} = 0, \quad S(t) \le x \le l,$$

where

$$q_1 = -\frac{\rho C_p \upsilon}{\lambda}; \quad p_1 = \frac{\rho C_p}{\lambda}$$
$$q_2 = -\frac{\rho_S C_{pS} \upsilon}{\lambda_S}; \quad p_2 = \frac{\rho_S C_{pS}}{\lambda_S}$$

ρ – melt density;

C_p – specific heat capacity of melt;

λ – coefficient of melt heat conductivity;

v – pulling rate of composite.

Initial conditions: $S(0) = S_0 > 0$ – given on interval (0, l) number;

$T_1(x, 0) = T_1(x)$,

$T_2(x, 0) = T_l(x)$ – given initial values of desired functions

$T_1(0, t) = T_0$,

$T_2(l, t) = T_l$ – given values of desired functions at the ends of interval $0 \le x \le l$.

Apart from this, at $x = S(t)$ let's require a fulfillment of conditions of consistency:

$T_1[S(t), t] = T_2[S(t), t] \equiv T^*$,

where T^* - given number.

Let's designate

$v_{11}(\tau) = T_1[0, \tau]$, $v_{12}(\tau) = T_1[S(\tau), \tau]$,

$v_{21}(\tau) = T_2[S(\tau), \tau]$, $v_{22}(\tau) = T_2[l, \tau]$.

$\mu_{11}(\tau) = \partial/\partial\xi \, T_1[0, \tau]$, $v_{12}(\tau) = T_1[S(\tau), \tau]$,

$v_{21}(\tau) = T_2[S(\tau), \tau]$, $v_{22}(\tau) = T_2[l, \tau]$.

$$\mu_{11}(\tau) = \frac{\partial}{\partial \xi} T_1(\xi, \tau) \Big|_{\xi=0} + \nu_{11}(\tau)[0 - q_1],$$
$$\mu_{12}(\tau) = \frac{\partial}{\partial \xi} T_1(\xi, \tau) \Big|_{\xi=S(t)} + \nu_{12}(\tau)[S(t) - q_1];$$

$$\mu_{21}(\tau) = \frac{\partial}{\partial \xi} T_2(\xi, \tau) \Big|_{\xi=S(t)} + \nu_{21}(\tau)[S(\tau) - q_2],$$
$$\mu_{22}(\tau) = \frac{\partial}{\partial \xi} T_2(\xi, \tau) \Big|_{\xi=l} + \nu_{22}(\tau)[0 - q_1];$$

$0 < \tau \le t$.

Let's introduce function

$$g_1(\xi,t_1)=\frac{1}{2\sqrt{\pi t_1}}\left\{\exp\left[\frac{q_1}{2}\xi+t_1\frac{q_1^{\,2}}{4\rho_1}+\frac{\xi^2\rho_1}{4t_1}\right]\right\}^{-1}, \tag{2.3.1}$$

which meets the equation

$$\frac{\partial^2 g_1}{\partial\xi^2}+q_1\frac{\partial g_1}{\partial t}=0. \tag{2.3.2}$$

Indeed,

$$\frac{\partial g_1}{\partial\xi}=-\frac{1}{2\sqrt{\pi t_1}}\left\{\exp\left[\frac{q_1}{2}\xi+t_1\frac{q_1^{\,2}}{4\rho_1}+\frac{\xi^2\rho_1}{4t_1}\right]\right\}^{-1}\cdot\left[\frac{q_1}{2}+\frac{\xi\rho_1}{2t_1}\right]$$

$$\frac{\partial^2 g_1}{\partial\xi^2}=\frac{1}{2\sqrt{\pi t_1}}\left\{\exp\left[\frac{q_1}{2}\xi+t_1\frac{q_1^{\,2}}{4\rho_1}+\frac{\xi^2\rho_1}{4t_1}\right]\right\}^{-1}\cdot\left[\left(\frac{q_1}{2}+\frac{\xi\rho_1}{2t_1}\right)^2-\frac{\rho_1}{2t_1}\right];$$

$$\frac{\partial g_1}{\partial\xi_1}=-\frac{1}{2t_1}\frac{1}{2\sqrt{\pi t_1}}\left\{\exp\left[\frac{q_1}{2}\xi+t_1\frac{q_1^{\,2}}{4\rho_1}+\frac{\xi^2\rho_1}{4t_1}\right]\right\}^{-1}-\frac{1}{2\sqrt{\pi t_1}}\left\{\exp\left[\frac{q_1}{2}\xi+t_1\frac{q_1^{\,2}}{4\rho_1}+\frac{\xi^2\rho_1}{4t_1}\right]\right\}^{-1}\left[\frac{q_1^2}{4\rho_1}-\frac{\xi^2\rho_1}{4t_1}\right].$$

Substituting in (2.3.2), we obtain

$$\frac{1}{2\sqrt{\pi t_1}}\left\{\exp\left[\frac{q_1}{2}\xi+t_1\frac{q_1^{\,2}}{4\rho_1}+\frac{\xi^2\rho_1}{4t_1}\right]\right\}^{-1}\cdot\left[\frac{q_1^2}{4}+\frac{q_1\xi\rho_1}{2t}+\frac{\xi^2\rho_1^2}{4t_1^2}-\frac{\rho_1}{2t_1}-\frac{q_1^2}{2}-\frac{q_1\xi\rho_1}{2t_1}+\frac{\rho_1}{2t}+\frac{q_1^2}{4}-\frac{\xi^2\rho_1^2}{4t_1^2}\right]=0.$$

Applying partial integration and use equality

$$\frac{d}{d\tau}\int_0^{S(\tau)}g_1(\xi-x,t-\tau)T_1(\xi,\tau)d\xi=\int_0^{S(\tau)}\frac{\partial}{\partial\tau}\{g_1(\xi-x,t-\tau)T_1(\xi,\tau)\}d\xi+S(t)g_1[S(\tau)-x,t-\tau]\nu_{12}(\tau),$$

$$\frac{d}{d\tau}\int_{S(t)}^{\rho}g_2(\xi-x,t-\tau)T_2(\xi,\tau)d\xi=\int_{S(t)}^{l}\frac{\partial}{\partial\tau}\{g_2(\xi-x,t-\tau)T_2(\xi,\tau)\}d\xi-\dot{S}(\tau)g_2[S(\tau)-x,t-\tau]\nu_{21}(\tau),$$

we obtain integral representation of arbitrary decision of Stephan's problem in a form:

$$T_1(x,t)=T_1^{H'}(x,t)+T_1^1(x,t)+T_1^2(x,t),$$

where

$$T_1^H(x,t) = \int_0^{S_0} T_1(\xi,0)\cdot g_1(\xi - x, t_1)d\xi,$$

$$T_1^1(x,t) = -\int_0^{t_1} \mu_{11}(\tau)\cdot g_1(-x, t_1-\tau)d\tau + \int_0^{t_1} \mu_{12}(\tau)\cdot g_1[S(\tau)-x, t_1-\tau]d\tau,$$

$$T_1^2(x,t) = -\int_0^{t_1} \nu_{11}(\tau)\frac{d}{dx} g_1(-x, t_1-\tau)d\tau + \int_0^{t_1} \nu_{12}(t)\frac{d}{dx} g_1[S(\tau)-x, t_1-\tau]d\tau;$$

$$T_2(x,t) = T_2^{H'}(x,t) + T_2^1(x,t) + T_2^2(x,t),$$

where

$$T_2^H(x,t) = \int_{S_0}^{l} T_2(\xi,0)\cdot g_2(\xi - x, t_2)d\xi,$$

$$T_2^1(x,t) = -\int_0^{t_2} \mu_{21}(\tau)\cdot g_2(S(\tau)-x, t_2-\tau)d\tau + \int_0^{t_2} \mu_{22}(\tau)\cdot g_2(l-x, t_2-\tau)d\tau,$$

$$T_2^2(x,t) = -\int_0^{t_2} \nu_{21}\frac{d}{dx} g_2[S(\tau)-x, t_2-\tau]d\tau + \int_0^{t_{21}} \nu_{22}(\tau)\frac{d}{dx} g_2(l-x, t_2-\tau)d\tau.$$

Thus the apparatus to resolve this problem is developed and we need to make the next step – to apply it for solution of definite problems realizing the technology of directed solidification for eutectic systems LaB_6-MeB_2. This a rather complicated problem and its solution is also allocated for the next project.

2.4. CALCULATION OF PHYSICO-MECHANICAL CHARACTERISTICS OF INVESTIGATED COMPOSITES

Let's consider a model object which is maximum close to technological sample obtained by the method of directed solidification.

Let's consider a cylinder with typical sizes of L, S and appropriate mechanical characteristics of matrix and inclusions (E – Young modulus, ν - Poisson's ratio), which suffers given external deformation and also can be used in cooling mode (temperature difference) encountering thermo-deformations, is considered.

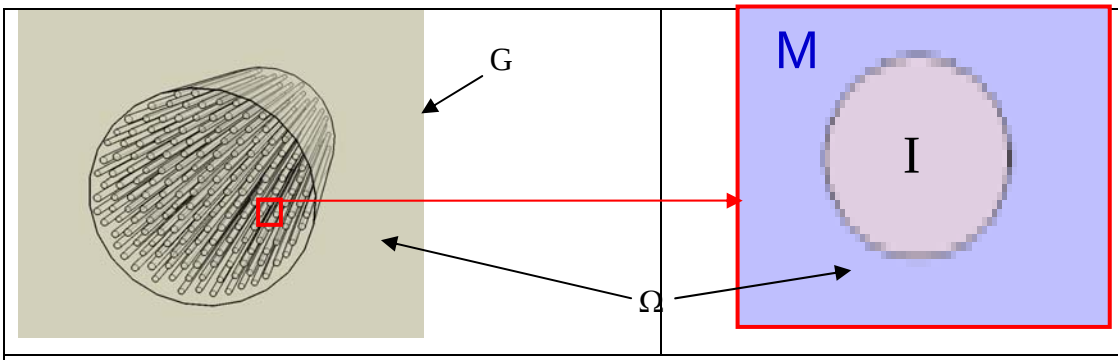

Fig.2.4.1. Geometrical model of material. I – MeB_2 intrusion (fiber), M – LaB_6 matrix, surface G - boundary of the sample, Ω - 3-D area representing a sample

Algorithm of calculation of mechanical properties is based on asymptotic method of averaging by Bashvalov-Sanches Palencia [44], [45], i. e. in some area Ω correspondent to a sample of the investigated material, thus a boundary problem is considered as:

$$\sum_{j=1}^{3} \frac{\partial \sigma(\vec{x})_{ij}}{\partial x_j} = 0; \qquad (2.4.1)$$

i, j, k, l=1,2,3

$$\sigma_{ij}(\vec{x}) = \sum_{k,l=1}^{3} C_{ij}^{kl}(\vec{x}) \varepsilon_{kl}(\vec{x}), \qquad (2.4.2)$$

where $\sigma_{ij}(\vec{x})$ - local stresses, $C_{ij}^{kl}(\vec{x})$ - local modules of elasticity and local deformations $\varepsilon_{ij}(\vec{x})$ are defined through displacements $\vec{u}(\vec{x})$:

$$\varepsilon_{ij}(\vec{x}) = \frac{1}{2}\left(\frac{\partial u_i(\vec{x})}{\partial x_j} + \frac{\partial u_j(\vec{x})}{\partial x_i} \right). \qquad (2.4.3)$$

Boundary conditions (2.4.1)-(2.4.3) are given as:

$$\vec{u}(\vec{x}) = 0, \quad x \in \Gamma_1; \qquad (2.4.4)$$

i, j=1,2,3

$$\sum_{i=1}^{3} \sigma_{ij}(\vec{x}) n_j = F_i(\vec{x}), \quad x \in \Gamma_2, \qquad (2.4.5)$$

where Γ_1 and Γ_2 - boundaries of area Ω, and $\vec{F}(\vec{x})$ - given force field, applied to area surface.

Let's find a solution of the above said problem as:

$$u_i(\vec{x}) = \sum_{j=1}^{3} e_{ij} x_j + w_i(\vec{x}, \hat{e}), \qquad i, j=1,2,3 \qquad (2.4.6)$$

where e_{ij} - components of tensor of external (macroscopic) deformations $\hat{e}$, and functions $w_i(\vec{x}, \hat{e})$ are periodic on representative cell of material. In linear approximation we obtain:

$$w_i(\vec{x}, \hat{e}) = \sum_{p,q=1}^{3} e_{pq} w_i^{pq}(\vec{x}), \qquad (2.4.7)$$

where $w_i^{pq}(\vec{x})$ - symmetrical on p, q and are solutions of six systems of equations:

$$\sum_{i,k,l=1}^{3} \frac{\partial}{\partial x_i} \left(C_{ij}^{kl} \left(e_{kl}^{pq} + \frac{1}{2}\left(\frac{\partial w_k^{pq}}{\partial x_l} + \frac{\partial w_l^{pq}}{\partial x_k} \right) \right) \right) = 0 \qquad (2.4.8)$$

for six linearly-independent single external deformations e_{ij}^{pq} (three one-axis compressions and three displacements). Thus the effective modules of elasticity $\tilde{C}_{ij}^{kl}$ are defined by integrals:

$$\tilde{C}_{ij}^{pq} = \int_V \sum_{k,l=1}^{3} C_{ij}^{kl} \left(e_{kl}^{pq} + \frac{1}{2}\left(\frac{\partial w_k^{pq}}{\partial x_l} + \frac{\partial w_l^{pq}}{\partial x_k} \right) \right) dV \qquad (2.4.9)$$

on volume of a representative cell.

Thus, for given distribution of elasticity modules by the area of representative cell the system of equations (2.4.8) was numerically solved on 3d net to compute $w_l^{pq}(x)$ in each node of the cell. Then integral (2.4.9) over the cell was used compute effective elasticity modules, and for given “macroscopic” deformation e_{ij} equations (2.4.4), (2.4.5) were used to compute local details of deformations. Then simple counting (due to discrete form of the problem after applying the grid) allowed compute distribution of deformations in a cell per volume unit independently for matrix and inclusion.

A number of materials base on LaB_6 matrix were simulated as infinite space filled by parallel round cylinders with axes passing through nodes of 2d periodic net. This geometry reasonably corresponds to the structure of materials in scope, example of which is represented on photo on fig 2.4.2 - fibers have approximately same diameter and placed uniformly, with no significant concentration.

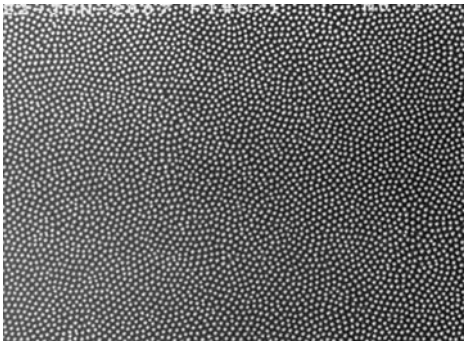

Fig.2.4.2 Microstructure of LaB_6-ZrB_2 sample

The requirement to initial melt to be eutectic specifies components concentrations in the material. Observation (uniform distribution of sizes and density of the fibers) allows to choose representative cell with single cylindrical inclusion of length which significantly exceeds it’s diameter. Specific concentration, relative placement and shape of fibers define uniquely possible ratios of linear sizes in the representative cell. Thus, ratio of typical distance between centers of the fibers (in the model in scope – linear size of representing cell) to their diameters is defined by solidification conditions, that mean they correspond to volume concentration of the fibers material in eutectic of the melt.

Initial data used to compute effective modules of a number of materials LaB_6-MeB_2 are presented in Table 2.4.1.

Table 2.4.1 Initial data: E – Young's modules, x_{mass} – mass share, MeB_2 ρ_g / ρ_m - ratio of inclusions density to matrix one, c_{vol} – volume share, calculated by formula $c_{vol} = x_{mass}\,\rho_m / \rho_g$; α_g / α_m – ratio of coefficients of volume expansion of inclusion and matrix. Young's modules for LaB_6 is accepted as $E=4{,}88 \times 10^{11}$ Pa.

	HfB_2	**NbB_2**	**TaB_2**	**TiB_2**	**ZrB_2**
E x 10^{-11}Pa	4.7971	6.736	6.867	5.4053	4.958

	LaB_6-HfB_2	**LaB_6-NbB_2**	**LaB_6-TaB_2**	**LaB_6-TiB_2**	**LaB_6-ZrB_2**
x_{mass}	0.220	0.202	0.324	0.103	0.210
ρ_g / ρ_m	4.25	2.61	4.27	1.72	2.08
c_{vol}	0.062	0.087	0.101	0.062	0.114
α_g / α_m	0.719	0.922	0.984	1.250	1.281

As a result of computing experiment to define mechanical characteristics of eutectic composites the following effective modules of elasticity are obtained and calculated by the above-described technique.

Table 2.4.2 Effective modules of elasticity of composites C_{ij} obtained at calculations, and Poisson's coefficient $\nu = C_{12} / (C_{12} + C_{11})$, Young's modulus $E = (C_{11} + 2C_{12})(C_{11} - C_{12}) / (C_{11} + C_{12})$ and shear modulus in plane (*x,y*) $\mu = C_{44}$.

	LaB_6-HfB_2	**LaB_6-NbB_2**	**LaB_6-TaB_2**	**LaB_6-TiB_2**	**LaB_6-ZrB_2**
C_{11} x 10^{-11}Pa	5.105	5.235	5.312	5.144	5.118
C_{12} x 10^{-11}Pa	0.827	0.845	0.856	0.833	0.825
C_{44} x 10^{-11}Pa	2.139	2.193	2.224	2.156	2.146
E x 10^{-11}Pa	4.874	5.000	5.074	4.912	4.889
ν	0.139	0.139	0.139	0.139	0.139
μ x 10^{-11}Pa	2.139	2.193	2.224	2.156	2.146

The well-known ideas of reinforcing of materials by nanotubular structures with the aim of introduction of their unique mechanical properties in operational characteristics of composites touched eutectics as well. In [46] it is shown, what even eutectic temperature for pseudo-binary eutectic systems TiN-AlN, TiC-TiB_2, TiN-NB_2 at reduction of characteristic linear size of inclusion up to 10-20 nm falls on $600 \div 900\,^0$C and in work [47] it is shown that Vickers's hardness for the system TiN-Si_3N_4-$TiSi_2$ at characteristic linear size of 3

nm reaches 100 GPa. It gives a hope that in case of realization of the technology of directed solidification an opportunity of achievement of nanosizes for diameters of fibers of inclusion of reinforced phase the obtained nanocomposites will possess very attractive mechanical properties.

At calculations for model LaB_6, reinforced by nanotubes, Young's modulus of nanotubes is accepted as 47.971×10^{11} Pa. Geometry of a material (and, thus a representative cell) are accepted the same as for eutectic alloys, but a ratio of nanotube radius and cell size varies in some limits, as requirements to observance of concentration equal to eutectic are absent. Table 2.4.3 includes the effective characteristics obtained as a result of calculations depending on bulk concentration of nanotubes on the stated algorithm and for comparison – values, average on composite volume.

Table 2.4.3 Effective and average on volume characteristics for LaB_6, reinforced by nanotubes, depending on bulk concentration of nanotubes

c_{vol}	**0.041**	**0.077**	**0.112**	**0.197**
effective on Bahvalov - Sanchez- Palencia				
C_{11}, C_{22}	6.552	7.805	9.066	12.082
C_{33}	6.955	8.548	10.140	13.923
C_{12}	1.040	1.219	1.399	1.827
C_{23}, C_{31}	0.996	1.139	1.284	1.634
C_{44}, C_{55}	$^{\cdot 11}$ 2.609	3.018	3.434	4.435
C_{66}	2.605	2.999	3.394	4.342
average on volume				
C_{11}	6.955	8.548	10.140	13.923
C_{12}	1.105	1.340	1.576	2.135
C_{66}	2.925	3.604	4.282	5.894

As it is seen from the table 2.4.3 a theoretical prediction shows a substantial growth of elastic constants, and control calculations of common average on volume values show a rather close results that means a qualifying character of Bahvalov - Sanchez- Palencia asymptotic technique.

To obtain a distribution of thermo-deformations we accepted the following assumptions:

1. Stresses in composite at temperature of crystallization are equal to zero
2. Coefficients of linear expansion of composite components are isotropic
3. Coefficients of linear expansion and modules of elasticity of components are constant and suffer a jump on interface inclusion – matrix.

Then the equation (2.4.3.) can be re-written as:

$$\varepsilon_{ij}(\vec{x}) = e_{ij} + \frac{1}{2}\sum_{p,q=1}^{3}\left(\frac{\partial w_i^{pq}}{\partial x_j} + \frac{\partial w_j^{pq}}{\partial x_i}\right)e_{pq} + \delta_{ij}\theta(\vec{x},T) \quad , \tag{2.4.10}$$

where $\theta(\vec{x},T)$ - piecewise-constant function of coordinates equal to zero when $T=T_m$: $\theta(\vec{x},T_m)=0$. In linear approximation on T $\theta(\vec{x},T)=\alpha(\vec{x})(T-T_m)$, where α - coefficient of linear expansion.

After substitution of equation (2.4.10) in (2.4.1&2.4.2) and their numerical solution regarding $\vec{w}^{pq}(\vec{x})$, under a condition of binding (the functions $u_i(\vec{x})=\sum_{j=1}^{3}\varepsilon_{ij}(\vec{x})x_j$ should be continuous) micro-distributions of thermo-deformations illustrated in figs. 2.4.3 & 2.4.4 are calculated.

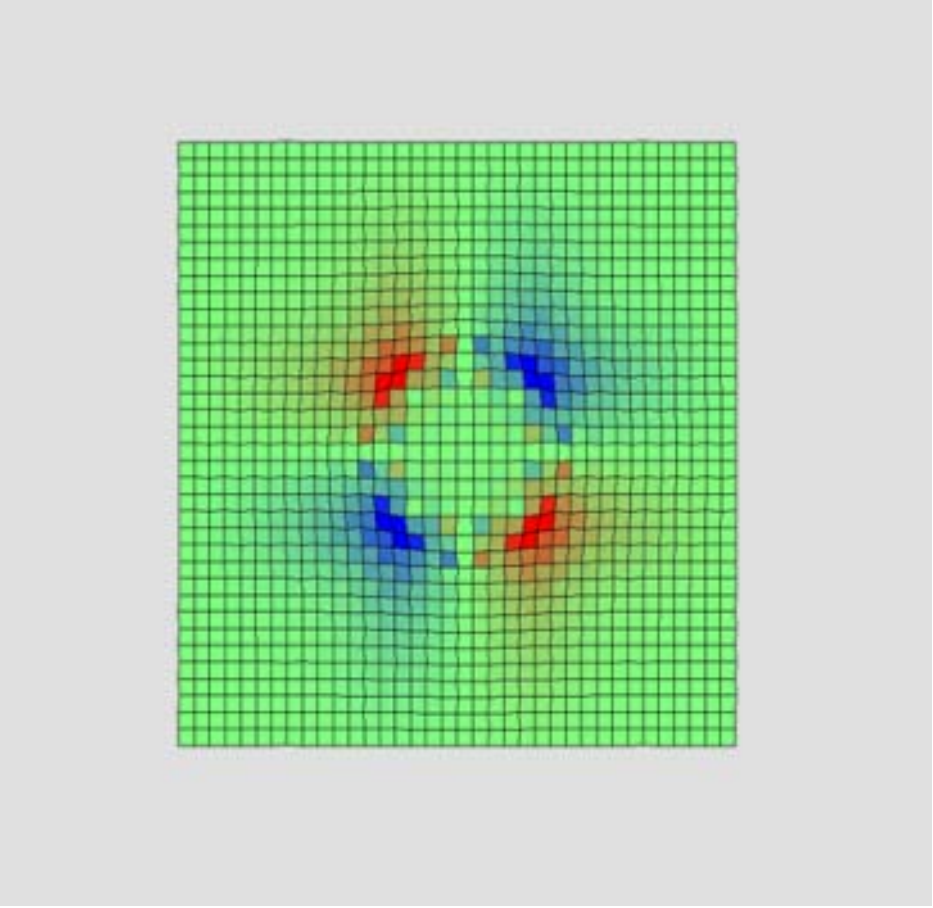

Fig. 2.4.3 Distribution shear component of thermo-deformations in representative cell of composite LaB_6-HfB_2. Green color corresponds to not deformed material. Intensity of red and blue colors corresponds to an intensity of shear in a plane, perpendicular to fiber axis, a color is defined by a sign of shear deformation

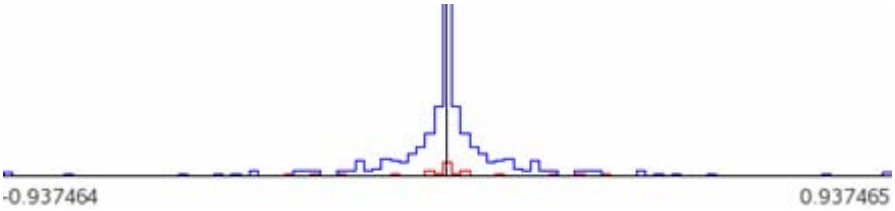

Fig 2.4.4 Distribution of a degree of shear component of deformation on volume. Blue curve – matrix LaB_6, red – fiber HfB_2

From the results of calculations it is clear that the most part of materials of matrix and inclusion suffers only weak internal deformations associated with composite matrix structure and only the area of matrix around fiber is strongly deformed.

3. Mesoscale. Multifractal analysis of images of fracture surfaces in scanning probe microscopy

Analysis of crystallization front – interface solid – liquid (gaseous) phase is usually carried out in terms of traditional description of an object by means of geometrical figures (lines, segments, polygons, etc.) which metrical and topological dimension is equal among each other. At the same time many geometrical forms, which were analyzed only at description level, now could be studied and described in strict quantitative terms of fractal approach proposed and developed by Madelbrot [48].

Processing of electron microscopic images is one of a key problem of materials science. To do that an apparatus of fractal geometry has recently been applied [49, 50]. Despite successful application of the above said technique for investigation for example, breaks [51], fractal analysis of materials structure has a number of restrictions, namely, sensitivity to deviation from fractality, etc. To overcome these inconveniences a method of multifractal analysis of images (MFA) was developed.

Multifractal description is based on generation of measure (by this or that way) at space partition, embracing the object being investigated, on cells, i.e. transition from fractal to multifractal description means thereby a transition from investigation of only geometrical structure to investigation of measure.

All operations of mathematical morphology applied for analysis of images are ways to extract the information of image. The approach early developed [52] to use the information of transformation for computer processing of images of materials structure enables to perform multifractal parameterization of different elements of structure, since various types of influences on material are appeared in changing of fractal (multifractal) structure of elements of material (grain boundaries, subgrains), microstructure (phase distribution, etc.), microcrack profile at its growth, distribution of pores and microcracks at a stage of pre-fracture, break design, surface profile, etc. As it's known, the realized symmetry of fractal structures (F-symmetry) in objects depends on external conditions. It defines a character of self-similarity, i.e. one should consider a set as fractals (multifractals), which in a process of evolution degrades in monofractal. For multifractal sets, use of one structure characteristic – fractal dimension – is not sufficient, and requires defining a grade of homogeneity and other characteristics.

Natural fractals like colloid aggregates, aero gels, clouds, polymers, porous mediums, dendrites, cracks, fracture surfaces of solid bodies, etc possess only by static self-similarity which may exist at that only in limited interval of space scales $L_0<L<L_m$. These objects are called as multifractals, since they can be represented as a set of fractal structures weighted with various weight. Rigorously proven, that d_q is not increasing function q, thus $d_{q+1} \le d_q$. At that $d_0=d_f$ – fractal dimension characterizing metrical properties of structure, $d_1=d_1$ – informational dimension describing a behaviour of Shannon's informational entropy $I(\varepsilon)=\sum_i^M P_i \ln P_i$, $a\ d_2 = d_c$ - correlation dimension, associated with internal energy U of multifractal structure.

Fundamental act of information processing is a comparison of elements of characteristics set as direct images of real objects or systems in information storage devices are represented by a number of quantitative characteristics [52]. Information is understood as a set of discrepancies of these characteristics compared by this or that way in terms of one or several sets.

In a framework of developed methodology [52], a mathematical object (measure) was subjected to group multifractal transformation to define which form of F-symmetry it possesses. If as a result of transformation the object does not change, then it possesses F-symmetry, in case it does then F-symmetry is violated and one may define a degree of it's violation.

Let's consider some investigated object immersed in Euclidean space and let's divide it on N equal cells with size 1 (equal-cell partition). Let's the object is described by measure $\{\mu_i = \mu(x_i)\}$, x_i — coordinates of I cell, $\sum_{i=1}^N \mu_i = 1$. Further we introduce transformation $\mu_i(q) = (\mu_1)^q / \chi(q)$, $\chi(q) = \sum_{k=1}^N (\mu_k)^q$, where $x(q)$ — so-called correlation function. When $q=1$, we obtain unit identity substitution. Since the measure $\{\mu_i = (q)\}$ fully coincides with own measure $\{\mu_i\}$, at any q only in case of uniform measure $\{\mu_i = \text{const}\}$, parameter q plays managing role, responsible for elevation of inhomogeneity of measure after transformation $\{\mu_i\} \to \{\mu_{1i}(q)\}$. This transformation represents a group, since for any transformation with definite parameter q_1 there is a reciprocal one with parameter $1/q_1$, recovering measure. Distribution $\{\mu_{1i}(q)\}$ should reflect peculiarities of own measure $\{\mu_i\}$, and one may investigate these peculiarities while comparing measure pre- and post transformation, using a partial form of information of transformation [52] — multifractal information as a measure of their discrepancy $I(q) = \sum \mu_i \ln(\mu_i / \mu_{1i})$. Simple calculation provides us

$$\lim_{l\to 0} \frac{I(q)}{(q-1)\ln l} = \frac{\tau(q)}{(q-1)} - D_1 = D_q - D_1,$$

or

$$D_q = D_1 + \lim_{l\to 0} \frac{I(q)}{(q-1)\ln l},$$

where D_1 — usual informational dimension, D_q — generalized dimensions (entropies) Reni.

$$D_q = \frac{\tau(q)}{(q-1)},\ \tau(q) = \lim_{l\to 0} \frac{\ln \chi(q)}{\ln l}.$$

From here (if to remind the rules of theory of limits) it's seen that multifractal information bonds all Reni's entropies $S(q) = \ln\left[\chi(q)\right]/(q-1)$ with information of Neumann – Shannon - Winner of initial measure $\sum \mu_i \ln \mu_i = S(1)$. More than that, difference of informational dimension with values of Reni's dimensions on "ends" of spectrum gives two evaluations of extremums of multifractal information (divided on $(q-1)$), which can be accepted as quantitative measure of order. Legandre's transformation of exponent of multifractal information

$$\tau_1(q) = \lim_{l\to 0} \frac{I(q)}{\ln l} = (q-1)(D_q - D_1)$$

provides definite parametric formulas of shifted $f(\alpha)$-spectrum. Thus, formulas of multifractal formalism are obtained at investigation of partial form of information of group transformation — multifractal information.

Application of these theoretical aspects for the goals of practical materials science is realized by means of creation of methodology and methods of multifractal parameterization of structures with flow automat processing of images of materials structures as digitized photos. Scanning probe microscopy (SPM) enables to investigate with high-resolution surface morphology in a broad range of magnifications [55]. However while analysing images obtained by means of SPM, there appear significant difficulties as a majority of methods applied for numerical estimation of surface roughness depends on scale of measurements. Unlike other characteristics of roughness fractal dimension is invariant value relatively to scale transformation. Definition of fractal distribution (FD) enables quantitatively to describe changing of material surface relief developing in a process of growth, loading, fracture [53], etc. However accuracy of definition of a value of fractal geometry to certain extent depends on method of fractal analysis and parameters of SPM images. FD values obtained by different methods for the same surface often can be found in broad interval [54]. Having two dimensional image of rough surface where point brightness defines height of this point above null level one may fairly accept this image as three dimensional one, considering a value of brightness as additional coordinate. Having a value of height of section level, one may judge about a perimeter L on the amount of points with given brightness and about area A on the amount of points which brightness is higher than given value.

These methods and algorithms with criteria of spectrum selection were realized as computer program MFRDom.

The above said program is for Windows 95. It enables to process sets of black & white, grey & colour images of 2000x2000 pixels and diapasons of values q [-200, +200]. This software is developed on the base of experience gained in numerical multifractal analysis of images of structures of metals and alloys during a number of years. MFRDom calculates spectrums by two ways using the method of generation of measures of rough partition (MGMRP), allows to investigate spectrums in a mode of game establishing random selection of scales, accumulates values of required parameters of spectrums together with the results of statistical processing of correct spectrums in tables. The program records on disk all calculations results both test files for further processing by another processors or electronic tables. It was tested on model objects like direct lines Serpinsky's carpet and gives exact values of fractal dimension up to 4th (by the first way) and up to 8th (by the second technique) digit.

As it was above mentioned, the program MFRDom calculates spectrums by two ways. Let's briefly explain these ways below. The first way is to calculate multifractal characteristics, using a set of rough partitions with their measures then for each partition we can calculate generalized correlation function $\chi_k(q) = \sum_{i=1}^{N_k} \mu_{ik}^q$ for all given values *q* from certain diapason. Having design the analog of Richardson graph in two logarithmic axises $\ln l_k - \ln(\chi_k(q))$ for each generalized correlation function, and to define its inclination by the method of least squares we obtain evaluation of exponent of generalized correlation function $\tau(q)$,

$$\tau(q) = \frac{\partial \ln(\chi_k(q))}{\partial \ln l_k},$$

that is similar to use of L'Hospital rule.

Numerically having built function $\tau(q)$ for some diapason (the broader is the better) of values *q*, taken with given frequency (the often is the better), we may further, numerically take a derivative $d\tau/dq = \alpha(q)$, to calculate $f(\alpha)$-spectrum, $f(q) = qd\tau/dq - \tau(q)$, and spectrum of Rein's dimensions D_q, $D_q = \tau(q)/(q-1)$, $D_1 = \alpha(q=1)$.

The second way is analogue to direct definition of $f(\alpha)$-spectrums and consists of calculations of sums

$$A_k = \sum_i \mu_{1ik}(q)\ln(\mu_{ik}(q)),\ F_k(q) = \sum_i \mu_{1ik}(q)\ln(\mu_{1ik}(q)),\ \mu_{1ik}(q) = \frac{(\mu_{ik})^q}{\chi_k(q)}$$

for each rough partition on cells with size $(l_k)^d$ of elementary cells for all given values *q* from some diapason and definition of inclinations of dependencies A_k and F_k *vs* $\ln l_k$ for each used value *q* by the method of least squares

$$\alpha(q) = \frac{\partial A_k(q)}{\partial \ln l_k},\ f(q) = \frac{\partial F_k(q)}{\partial \ln l_k}.$$

A distinction of this technique is in a way of generation of rough measures. By calculated values $\alpha(q)$ and $f(q)$ one may define Reni's spectrum of dimensions, $\tau(q) = q\alpha(q) - f(q)$, $D_q = \tau(q)/(q-1)$, $D_1 = \alpha(q=1)$.

Results provided by MFRDom

D_1–D_{40}	Evaluation of measure of violation of fractal symmetry
F_{40}	Evaluation of quantitative measure of system homogeneity F_∞
D_{-40}–D_{40}	Difference of generalized Reni's dimensions
D_{-40}	Generalized Reni's dimensions ($D_q = \tau(q)/(q-1)$)
D_0	Fractal dimension $D_0 = -\tau(0)$
D_1	Informational dimension $D_1 = \lim_{q\to 1} \frac{\tau(q)}{q-1}$
D_2	Correlation dimension $D_2 = \tau(2)$
D_{40}	Generalized Reni's dimensions ($D_q = \tau(q)/(q-1)$)
F_0, F_1	$f(\alpha)$-spectrums; $f(q) = q\alpha(q) - \tau(q)$.
Alf_0, Alf_1, Alf_{40}	Scaling value $\alpha(q) = d\tau/dq$

Employment of generalized dimensions for quantitative description of structure MFT enables to define:

1) A degree of structure order on value of parameter $\Delta q^* = D_1 - D_{q^*}$. Value $\Delta q < 0$ characterizes absence of F-symmetry.
2) A change of set sparseness (density) at achievement of ultimate state (degradation of multifractality) on value of parameter $\delta_d = D_{q^*} - D^N_{q^*}$, where $D^N_{q^*}$ - ultimate value D_{q^*}, above which spontaneous change of type occurs: fractal with given F-symmetry, controlling fractal's degradation.
3) Index of adaptive properties of material's structure to external influence $A = \delta^N_\alpha / \left(\delta^N_\alpha\right)_{\max}$ where δ^N_α - achievable maximum density of set at its degradation into fractal with given F-symmetry.

As it was noticed, the program MFRDom is assigned for computer realization of multifractal processing of images with the use of algorithms of automatic selection of scales and statistic analysis of canonic pseudo spectrums.

As a model to check applicability of MFRDom to process real images of breaks we used Serpinsky's carpet (see fig. 3.1), for which exact fractal characteristics are known.

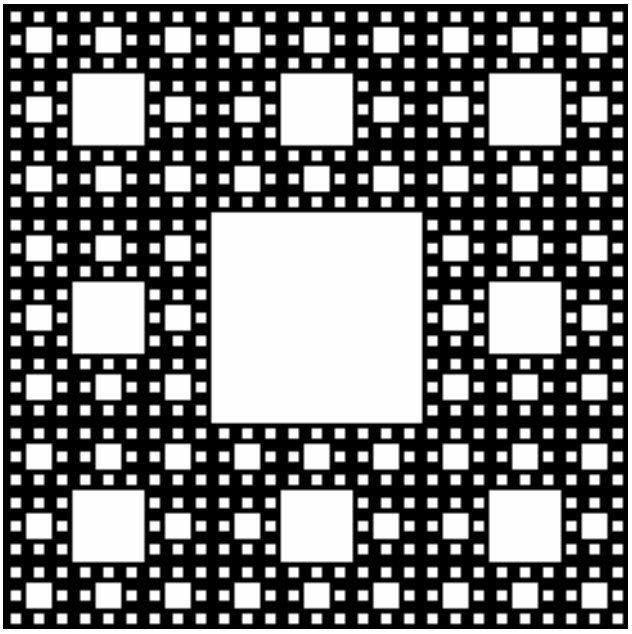

Fig. 3.1 Testing model - Serpinsky's carpet

Falling from a fact that the program cannot process images higher than 2000×2000 pixels, we choose 729×729 pixels (maximum degree 3, not exceeding 2000) for model image. Variants with carpet images with a size not degree 3 were not considered on grounds that this image would be automatically slightly distorted that would bring to additional unaccounted errors.

Images of real objects can be considered as distorted images of model objects that's why our work is to consider an influence of various distortions of ideal model image (Serpinsky's carpet) on the results of calculations of MFRDom program. The program calculates a lot of fractal characteristics of images, however the most representative and understandable is fractal dimension D_0, thus for the first turn we considered this particular value.

In case of ideal Serpinskiy carpet (see fig. 3.1) calculated values (both fractal dimension and other fractal parameters) coincide with theoretical ones ($D_0 \approx 1.893$).

Further we introduced a number of errors in the carpet.

1. The first modification of the carpet — transformation of image in negative. Here we obtained a rather unexpected result — carpet's structure remains fractal at the same rate as early, the calculated fractal dimension turned equal $D_0 \approx 1.906$. The program has adjustment what color — black or white— should be considered as a basic one (this change brings to correct result for fractal dimension of the carpet).

2. Further, since images of real objects may have random size, orientation and position on image, we investigated influence of cyclic shifting of the carpet relatively to centered position on calculation results (fig. 3.1 shows initial Serpinskiy carpet, and fig. 3.2 — shifted on 181 pixel on vertical). It was found out that for bigger amount of shiftings (55.5%) the program as calculated fractal dimension returns value 0; for the rest cases 44.5% the value of fractal dimension varies from 1.893 to 1.930, thus the exact value

1.893 is obtained only for 2.5% cases. The results for shifting on horizontal, as was expected, are identical to those results at shifting on vertical.

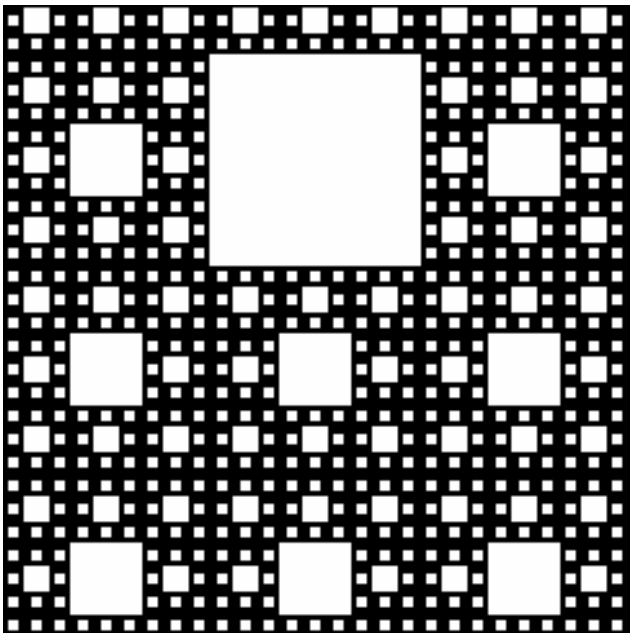

Fig. 3.2. Shifted Serpinskiy carpet

3. Next introduction of distortions included rejection of the same amount of lines from the right and bottom of the image (fig. 3.3 showed Serpinskiy carpet with rejected 54 lines from the right and bottom). We rejected from 1 up to 243 lines. It was found out that for a bigger amount of shiftings (57%) the program as calculated fractal dimension returns value 0; in the rest 43% cases the value of fractal dimension varies from 1.880 to 2.000.

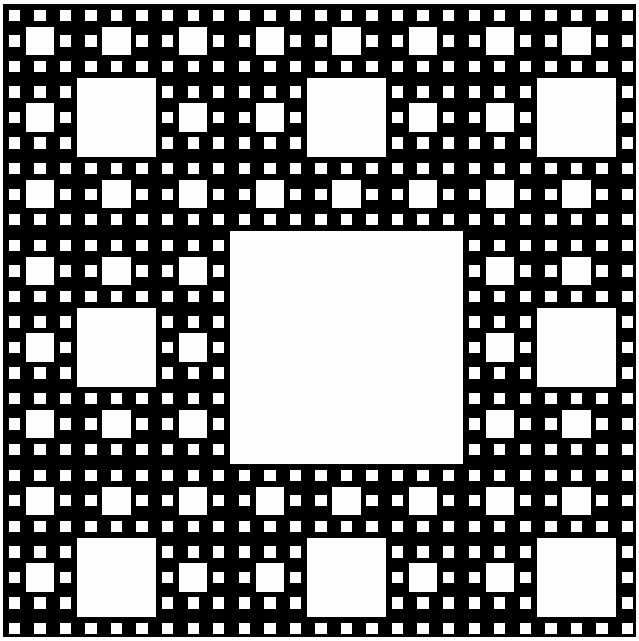

Fig. 3.3. Cut off Serpinskiy carpet

Unfortunately the obtained results witness that application of averaging of calculation results on a big number of images may turn unjustified. This is confirmed by the results of our next experiment.

4. From the model Serpinskiy carpet with size 729×729 we randomly cut off a square fragment 243×243, for which calculations were carried out. It came to light that in a majority of cases the program returned value $D_0 = 0$.

5. The results of experiment on blackening of separate white squares of carpet (one per image) were obtained. The program calculated all images; fractal dimension varied from 1.893 (square with size of 1 pixel) up to 1.909 (square size 243×243). However a value of this experiment is not that high due to impossibility of theoretical evaluation of fractal dimension of this model.

6. Having proceeded to discuss applicability of the program for calculation of fractal characteristics, let's note, that, since the program transform images in bicolor ones, assignment of frames of transformation white – black would be essentially influence on calculation results.

7. A dependence of fractal dimension from (amount) number of iteration while constructing Serpinskiy carpet was also investigated. For the carpet 243x243 the following results were obtained: 2 – for iteration under the number 1, 1.893 – for iteration by numbers 2, 3, 4 and 5. For the carpet 729x729: 2 – for iteration for 1, 1.893 – for iterations 2, 3, 4, 5 and 6.

8. "Spoiled" one bright square at each level (starting from the biggest carpet) in the right corner for the carpet 243x243. We obtained the following results: 1 level - 1.893, 2 level - 1.894, 3 - 1.901, 4 - 1.907.

9. Painted the same square at each level (location of square does not change depending on level number); for the carpet 27x27 - 1.907, 81x81 - 1.894, 243x243 - 1.893 and for 729x729 - 1.893.

The results obtained confirm that in a number of cases small distortions not touching a fractal nature of image (for example cyclic shear), may bring to values essentially differ from theoretical ones. More than that, as it's found out, application of averaging of calculated results on big number of images may also be unjustified.

In the whole variety of modern means for receiving of digital images, required for multifractal analysis, a researcher has to clearly represent parameters at scanning or photographing, at which he/she obtains these images. So, obtained in the above said experiments correlation dependencies of multifractal parameters with grain size of metal is built on images transferred to digital ones by scanning with density (resolution) 300 pixels/inch. However the use of other parameters at scanning would have brought a researcher to completely another results.

There are some important circumstances, which should be taken into account while caring out fractal analyse of images obtained by SPM. Due to that SPM needle has a final size, it cannot penetrate surface roughness, which sizes are less than some certain limit. That is why SPM image does not really copy surface relief of sample being investigated, and is its rather plane copy. As a result a value of fractal dimension of SPM image may vary from FD of real surface.

Due to a number of reasons SPM image of surface of solid bodies is always self-affine but not self-similar. First of all, for real physical objects roughness size in surface plane is usually bigger than those in perpendicular one. Secondly, SPM needle diapason in scanning plane as a rule is bigger than in

perpendicular direction. Due to self-affine, SPM images of surfaces of solid bodies may have only local fractal dimension. Thus for more reliable definition of FD value we need to investigate surface structure in local limit, i.e. with high resolution, when scanning step is small if compare with roughness size.

Since, self-affine surfaces are characterized only with local fractal dimension and are not fractal in global mean, then to define stable FD value one may only at investigation in certain diapason of magnification. As departing from this diapason, a fractal dimension of surface decreases and heads to topological one. To obtain reliable FD value characterizing surface, requires value D_f would remain constant at changing scanning scale at least on two-three orders.

Eventually, investigated surfaces of real objects are only statically self-affine. That is why FD value can not be unambiguously defined for certain sample and may vary on various parts of sample surface. We may speak only about average FD value, which is obtained by averaging of fractal dimensions calculated for different parts of sample surface.

Another factor, which may affect FD value, is the amount of points in SPM image. As a value of fractal dimension is defined by inclination angle of dependence $]nS/S_0$, then a reduction of points in image brings to decrease of a set of used values and eventually to reduction of points on a graph. The last may change graph inclination and thus change a value of fractal dimension. Apart from this, since a relief of different parts of surface may vary then a reduction of points leads to lesser stability of value *Df.* From the other hand, growth of points' number in image causes noticeable increase of time required for scanning and computer processing of images that rather complicates express analyses of sample surface. Thus, a necessity to define if there is a dependence of fractal dimension from image size and to define optimum size of image providing true value D_f appears.

A question about the influence of algorithm of transformation of image in digit format on calculation results is still open. Since the program transforms images in two color ones knowledge of threshold white-black may drastically affect on calculation results.

Photos shadiness may also affect on parameters of multifractal parameterization. In cases, when we analyze over etched structure or it is represented by dark components (pearlite, graphite), multifractal parameters are distorted.

Values of order $\Delta_{200} = D_1 - D_{200}$ (evaluation Δ_∞ - measure of violation of fractal symmetry) and homogeneity f_{200} (evaluation f_∞) influence on size of images being analyzed.

To investigate small disperse images one may recommend to use resolutions with divisor 3, as in this case values of multifractal parameters are minimum.

As an illustration of influence of preliminary processing of images on the obtained results let's bring examples of SPM images of real structures (see fig.3.4.).

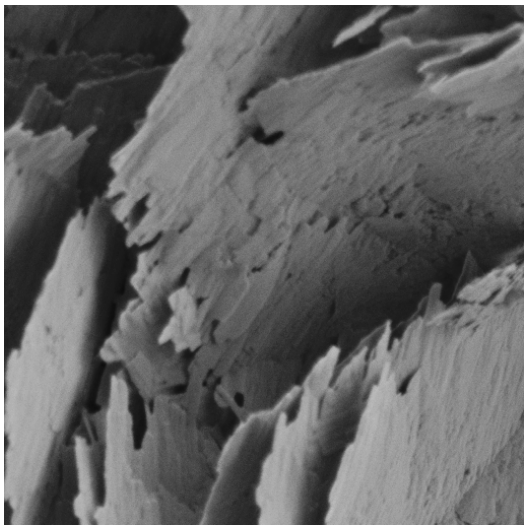

Scale 50000, image size 512x512.
Without processing: D_0=2.000; after transformation of image in “black & white”: D_0=1.872, D_1-D_{40}=-0.049, D_{-40}-D_{40}=-0.056, D_1=1.878, D_2=1.884, D_{40}=1.927

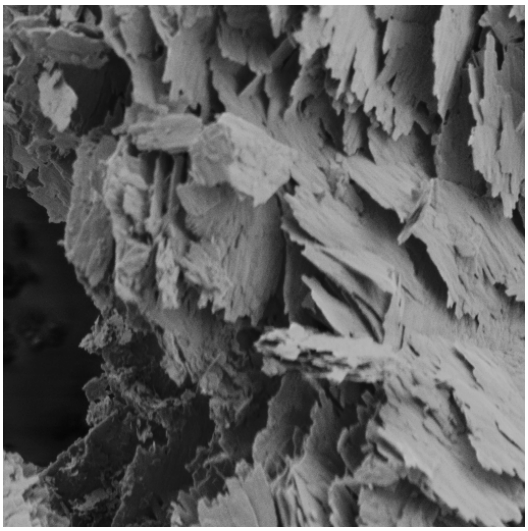

Scale 25000, image size 512x512.
Without processing: D_0=2.000; after transformation of image in “black & white”: D_0=1.885, D_1-D_{40}=-0.068, D_{-40}-D_{40}=0.151, D_1=1.890, D_2=1.895, D_{40}=1.958

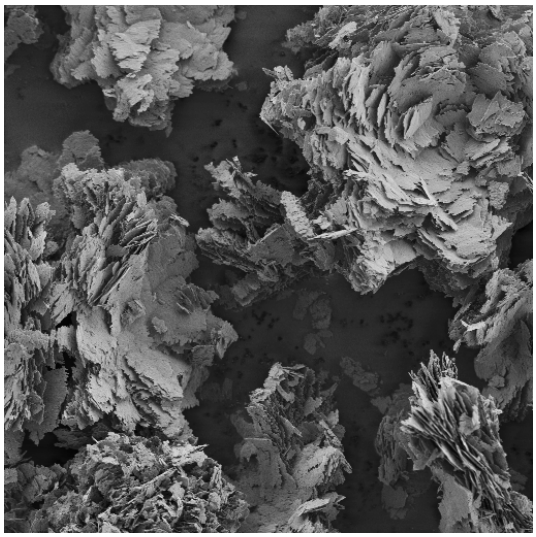

Scale 5000, image size 512x512.
Without processing: D_0=2.000; after transformation of image in “black & white”D_0=2.000, D_1-D_{40}= 0.144, D_{-40}-D_{40}=0.301, D_1=1.989, D_2=1.978, D_{40}=1.845

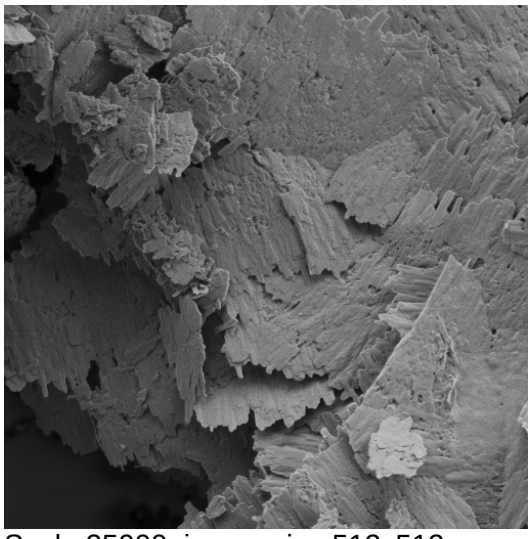

Scale 25000, image size 512x512.
Without processing: D_0=2.000; after transformation of image in “black & white”D_0=1.914, D_1-D_{40}=-0.052, D_{-40}-D_{40}=0.055, D_1=1.929, D_2=1.944, D_{40}=1.981

Fig.3.4. Samples of SPM images of real structures

Thus, the above offered technique of definition of multifractal characteristics of materials structure is based on analysis of images obtained by electron microscopy. Analysis of influence of distortions introduced in model fractal structures on multifractal characteristics of these structures obtained as a result of numerical experiment is carried out. This analysis showed that successful application of the method of multifractal analysis of images obtained by SPM unfortunately strongly depends on qualification and experience of a

researcher who carries this analysis. Our experience showed that as a rule, two researchers using the same set of SPM images obtain different values of multifractal characteristics. However if to accept a number of strict requirements for preparation of a package of analyzed images and to unify algorithms of calculation of multifractal characteristics then we would obtain a powerful method of quantitative characterization of structural parameters of investigated systems.

4. MICROSTRUCTURAL ASPECT OF A PROBLEM OF COMPUTER DESIGN OF EUTECTIC COMPOSITES IN SYSTEM LAB_6-MEB_2

4.1 PSEUDOPOTENTIAL METHOD OF CALCULATION OF TEMPERATURE AND CONCENTRATION OF COMPONENTS IN EUTECTIC POINT

One of the possibilities of modeling of phase equilibria in multicomponent systems is a thermodynamic calculation [56]. Usually to resolve this problem requires a set of experimental data, on which base one may calculate equilibrium phase composition in a broad temperature interval. Simulation results depend on reliability of basic experimental data. Any experimental information obtained by various researchers has a scattering associated with measurement device errors and chemical purity of investigated material in various cases. Experimental information is adequate, when the obtained results of a set of independent measurement processes meet each other. Modeling of phase equilibria of multicomponent systems from the first principles without required attraction of experimental information is very important for critical evaluation of experimental data available in literature, which contain a certain controversy.

To calculate characteristic parameters of eutectic systems as LaB_6 - MeB_2 one may use thermodynamic potentials built on the base of quantum – mechanical calculations.

A background of being investigated composite materials in the system LaB_6 - MeB_2 is made by lanthanum hexaboride (LaB_6) possessing with cubic structure like CaB_6, where a simple cube from metal atoms is centered by octahedron from boron atoms (see fig.4.1.1). Diborides of transitive metals have hexagonal structure of type AlB_2, where boron atoms form graphite-like nets perpendicular to axis Z, and the whole structure – subsequent alternation of hexagonal layers from metallic atoms located in units of hexagonal dense lattice with small ratio *c/a* and layers from boron atoms which form hexagonal two dimensional net (see fig.4.1.2) [57].

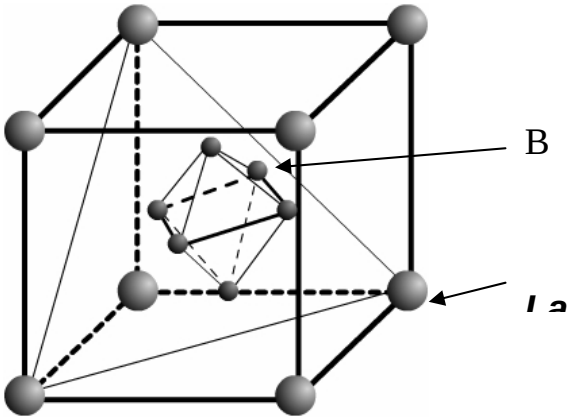

Fig. 4.1.1 Crystal lattice LaB_6

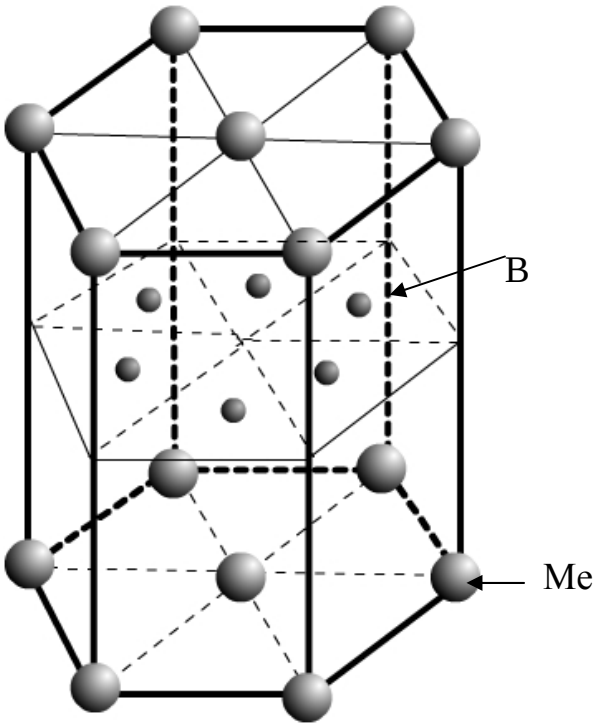

Fig. 4.1.2 Crystal lattice MeB_2

THERMODYNAMIC POTENTIAL

To describe a process proceeding at constant atmospheric pressure, a thermodynamic potential is used

$$F = U - TS\,, \tag{4.1.1}$$

where U - internal energy, *S* - entropy of system and T - absolute temperature.

Stable state of system under given conditions is a state with the lowest thermodynamic potential F.

Let's prove that on the base of components LaB_6 and MeB_2 quasi-binary systems of eutectic type may appear and let's define characteristic parameters (temperature, concentration) of these systems. Assuming that there are rather big single crystals (several angstroms) and for their description an employment of quantum-mechanical equations is justified. We consider only equilibrium state of solid solution on the base of two components for each system.

The following assumptions were made:

1.Composite material (LaB_6 - MeB_2) consists of two types of single crystals *A* (LaB_6) and *B* (MeB_2). The interface between two single crystals is chosen from geometrical considerations of coherence of crystalline lattices for two components A and B;

2. On interfaces of two different crystal lattices by virtue of smallness of local stresses responsible for incomplete correspondence of lattice parameters are not accounted for;

3. Energy of electron – ionic system is calculated per molecule using the second order perturbation theory by means of pseudopotential method;

If a crystal consists of similar atoms, then to calculate the energy of interatomic interaction a conception of volume per atom in crystal lattice is used. For crystals with complex structure a conception of average volume per atom in crystal lattice is incorrect. For these crystals a conception of representative cell instead of atom is introduced. Elementary cells consist of molecules, which volume coincides with cell volume. Considering that a complex structure is a crystal lattice with basis and all quantum-mechanical calculations carried out for atoms may be applied for molecules accounting for their mutual location.

4. Atoms interaction is accounted for only between closest neighbors in crystal lattice (1st coordination sphere);

5. System is equilibrium at constant volume.

Energy of electron-ion system in terms of pseudo-potential method in the second order of perturbation theory can be written as a sum

$$U = \frac{1}{N}\sum_{ij}\Phi(R_{ij}) \tag{4.1.2}$$

R_{ij} - distances between atoms *i* and *j*, *N*- number of atoms in system.

Pair of interatomic potentials is chosen as previously described [58]

На основе сделанных допущений энергию твердого раствора, приходящаяся на одну представительную ячейку с концентрацией C для компоненты А можно представить в виде:

$$U = C^2 U_{AA} + (1-C)^2 U_{BB} + C(1-C) U_{AB}, \qquad (4.1.3)$$

where U_{AA}, U_{BB}, U_{AB} - respectively energy of interaction between molecules A – A, B – B, and A – B , and a free energy we represent as [56]

$$F = C^2 U_{AA} + (1-C)^2 U_{BB} + C(1-C) U_{AB} - \frac{1}{N} k T S_{AB} - T\left[C S_A + (1-C) S_B\right], \qquad (4.1.4)$$

here k - Boltzmann's constant, S_A and S_B - components entropy, S_{AB} - entropy of components of mixing, N - total number of molecules in system.

To build thermodynamic potentials requires to define internal energy of system (energy electron – ion system). For calculation energy U electron-ion system a method of a priori pseudopotential is used [59].

DEVELOPMENT OF PSEUDO-POTENTIAL

If in complex structures made of molecules XY_n to combine the beginning of co-ordinates with atom X then atoms Y would be located on a distance $\left|\vec{\delta}_j\right|$, thus pseudo-potential can be presented as

$$V(q) = \frac{1}{\Omega_0}\left[\Omega_X V_X(q) + \Omega_Y V_Y(q) \sum_{i=1}^{n} \exp(-i\vec{q}\,\vec{\delta}_j)\right], \qquad (4.1.5)$$

where Ω_X, V_X and Ω_Y, V_Y volumes and pseudopotentials of atoms entering in composition, $\vec{\delta}_j$ - radius – vectors of atoms Y relatively atom adopted as the beginning of coordinates, Ω_0 - volume per molecule, n - number of atoms of the second component. In calculation we use a priori pseudopotential of type [59]

$$V(r) = -\frac{z}{r} + \sum_{l=0}^{l_0} (A_l + \frac{z}{r}) \exp(-r / R_l)\, P_l. \qquad (4.1.6)$$

Here l - orbital quantum number, l_0 - its maximum value for given atom, P_l - projection operator, A_l, R_l pseudopotential parameters (r - distance from electron to ionic shell).

Parameters of pseudo-potential A_l and R_l for presented elements are calculated by the methodology [59] and presented in table 4.1.1 (all values are in atomic units $\hbar = e = m = 1$).

Table 4.1.1 Parameters of pseudo-potentials (A_l and R_l) for investigated elements

	R_0	R_1	R_2	A_0	A_1	A_2

La	0,7045	0,6693	0,6456	5,11	5,647	6,05966
Ti	0,5439	0,5158	0,470	6,6176	7,3284	8,298
Zr	0,6335	0,5998	0,573	5,683	6,302	6,78098
V	0,520	0,500	0,468	6,923	7,56	8,33
Cr	0,495	0,477	0,446	7,27	7,924	8,744
B	0,258	0,192	-	12,99	19,69	-
Hf	0,523	0,497	0.477	6,88	7,61	8,174

Calculation of internal energy

Energy depending on structure type at constant molecule volume, would be a sum of electrostatic energy and energy of zone structure, which can be presented as a result of a sum of pair intermolecular potentials.

Pair intermolecular potentials for two molecules (i and j), distanced on R_{ij}, have a form

$$\Phi(R_{ij}) = \frac{2\Omega_0}{8\pi^3}\int [\,\Phi_0(\vec{q}) + \frac{2\pi}{\Omega_0 q^2}\,(z_1\frac{\Omega_1}{\Omega_0} + z_2\frac{\Omega_2}{\Omega_0}\sum_n \exp(-i\vec{q}\vec{\delta}_n))^2\,]\exp(i\,\vec{q}\vec{R}_{ij})\,d\vec{q}\ . \qquad (4.1.7)$$

Here z_1, z_2 - number of free electrons of atoms entering in molecules composition, $\Phi_0(\vec{q})$ - characteristic function

$$\Phi_0(\vec{q}) = V^2(q)\,\chi(q)\,\varepsilon(q)\,, \qquad (4.1.8)$$

where $\varepsilon(q)$ and $\chi(q)$ describe shielding and correlation of free electrons in investigated systems [58].

Energy of interaction of one type molecules U_{AA} or U_{BB} does not differ from analogous calculations for atoms and is defined by rearrangement of terms. Energy of molecules interaction can be presented as a sum of pair interatomic potentials,

$$U_{AA} = \frac{1}{N_0}\sum_{i,j}\Phi(\vec{R}_{ij}) \qquad (4.1.9)$$

where $\vec{R}_{ij}$ - distance between molecules i and j (N_0 - number of molecules in representative volume).

To calculate energies of interaction of various molecules let's make some simplifying steps. Let's chose molecule's average volume and charge, at presence of two types of molecules A and B, in a form

$$\overline{\Omega} = \frac{1}{2}(\Omega_A + \Omega_B); \quad \bar{z} = \frac{1}{2}(z_A + z_B)\,, \qquad (4.1.10)$$

where Ω_A, z_A and Ω_B, z_B represent volume and charge of molecules A and B.

Let's represent $\Phi_0(q)$ as

$$\Phi_0(q) = V_A(q)\,V_B(q)\,\bar{\chi}(q)\,\bar{\varepsilon}(q)\,. \qquad (4.1.11)$$

Here V_A and V_B pseudopotentials of molecules of type A and B, but $\overline{\chi}(q)$ and $\overline{\varepsilon}(q)$ functions accounting for exchange-correlation effects and shielding of free electron gas of averaged volume. Pair intermolecular potential for two types of molecules distance on R_{lj} can be written as

$$\Phi_{AB}(R_{lj}) = \frac{2\overline{\Omega}}{(2\pi)^3}\int_0^{2k_F}\left[\Phi_0(q) + \frac{2\pi}{\overline{\Omega}q_0^{\,2}}\overline{z}^2\right]\exp(i\vec{q}_0\vec{R}_{lj})\,d\,\vec{q}\,. \qquad (4.1.12)$$

Here $\vec{q}_0$ - wave vector for mixed structure. Averaging is carried out through numerical integration on q_0 in interval [0 – $2k^0{}_F$] ($k^0{}_F$ - Fermi impulse for averaged volume). Energy of interaction between molecules of type A and B let's write as

$$U_{AB} = \frac{1}{N}\sum_{l,j}\Phi_{AB}(\vec{R}_{lj})\,. \qquad (4.1.13)$$

Calculation of entropy

Components entropy can be defined by values of energy of thermal fluctuations of crystal lattice.

Average energy of fluctuation of crystal lattice [61]

$$\overline{U_T} = \sum_q \hbar\omega_q \Big/ ((\exp(\hbar\omega_q / kT) - 1)\,, \qquad (4.1.14)$$

where summation is carried out on all types of fluctuations (i.e. not only for all wave vectors $\vec{q}$, but for all polarizations).

Using Einstein's model [61], where all fluctuations are assigned with one frequency, at temperature T for energy of thermal fluctuations (per one molecule) we obtain

$$U_T = \frac{\hbar\omega}{\exp(\frac{\hbar\omega}{kT} - 1)}\,. \qquad (4.1.15)$$

Let's define a heat capacity C_Ω (at constant volume) [61] through energy of lattice oscillation

$$C_\Omega = \frac{k(\hbar\omega/kT)^2\exp(\hbar\omega/kT)}{((\exp(\hbar\omega/kT) - 1)^2}\,. \qquad (4.1.16)$$

Components entropy we define falling from [61] ratio

$$dS \cdot T = C_\Omega \cdot dT\,. \qquad (4.1.17)$$

Frequency of atoms oscillation ω is defined through power constants, which represent second derivatives from energy of interplane interaction on lattice parameter perpendicular to these planes.

Oscillation frequency is defined [59] by formula

$$\omega^2 = \frac{\alpha}{M}\,. \qquad (4.1.18)$$

Here $\alpha = \frac{\partial^2 E}{\partial c^2}$ at $c = c_0$ represents power constant, M - mass of molecule, E - energy of interplane interaction (c - lattice parameter perpendicular to oscillating planes, c_0 - its value in equilibrium state of crystal).

For calculation of energy of interplane interaction we represent a full potential as:

$$\Phi(R_{lj}) = \frac{2\Omega}{8\pi^3}\int\left[\Phi_0(q) + \frac{2\pi z^2}{\Omega q^2}\right]\cdot\exp(i\vec{q}\vec{R}_{lj})\,d\,\vec{q} \qquad (4.1.19)$$

Summarizing (4.1.9) on two parallel densely packed layers distanced from each other on h and displaced relatively each other on vector $\vec{\rho}$. In case MeB_2 $h = c/2$, $\vec{\rho} = 2\vec{a}/3 + \vec{b}/3$, where $\vec{a}$, $\vec{b}$ - vectors of basic plane, and $|\vec{a}| = |\vec{b}| = a$. E – energy of interaction between two planes (per surface unit) can be presented as follows:

$$E(h,\rho) = \frac{1}{S}\sum_{l,j}\frac{2\Omega}{4\pi^2}\int\left[\Phi_0(q) + \frac{2\pi z^2}{\Omega q^2}\right]\cdot\exp(iq_Z h)\cdot\exp(i\vec{q}_S(\vec{R}_{lj} + \vec{\rho}))\,d\,\vec{q}. \quad (4.1.20)$$

Here S - area per atom in densely packed layer, and vector $\vec{q}$ is decomposited on two components: $\vec{q}_S$ - on basic plane and q_Z - perpendicular to it.

For calculation of shift entropy we would fall from Boltzmann ratio

$$S = k\ln W,$$

where W, as it's known, represents a number of opportunities of realization of considered macroscopic state by means of exchange of molecules. We are only interested in additional opportunities appearing at the expense of displacement of components A and B. A number of these opportunities makes [63]

$$W = \frac{N!}{N_A!N_B!}. \qquad (4.1.21)$$

N_A, N_B - number of molecules A and B. Using Sterling's formula for bigger N, and introducing here value $C = N_A/N = 1 - N_B/N$, we obtain shift entropy

$$S_{AB} = -k[C\ln C + (1-C)\ln(1-C)]\cdot N\ . \qquad (4.1.22)$$

EUTECTIC FORMATION AND CALCULATION ITS CHARACTERISTIC PARAMETERS

After substitution of expressions for components entropy S_A, S_B and S_{AB} in formula (4.1.3), thermodynamic potential for investigated alloys in system $A-B$ for solid phase has a form

$$\begin{aligned} F\ &= C^2U_{AA} + (1-C)^2U_{BB} + 2C(1-C)U_{AB} + Tk\left[C\ln(C) + (1-C)\ln(1-C)\right] - \\ &T\left\{C[(1 + \frac{1}{\exp(\hbar\omega_A/kT) - 1})\hbar\omega_A/kT\ - \ln\left|exp(\hbar\omega_A/kT) - 1\right|]\right. \\ &\left. + (1-C)[(1 + \frac{1}{\exp(\hbar\omega_B/kT) - 1})\hbar\omega_B/kT - \ln\left|exp(-\hbar\omega_B/kT) - 1\right|]\right\}. \end{aligned}$$

Thus we obtained a functional dependence of thermodynamic potentials of composite materials from concentration and temperature. It's generally accepted that thermodynamic potential for ultimate case of insolubility in solid state degenerates in a straight line for all compositions from c=0 to c=1 [64]. Calculated dependence of thermodynamic potential from concentration in terms of quantum-mechanical theory differs from linear law (see fig.4.1.3).

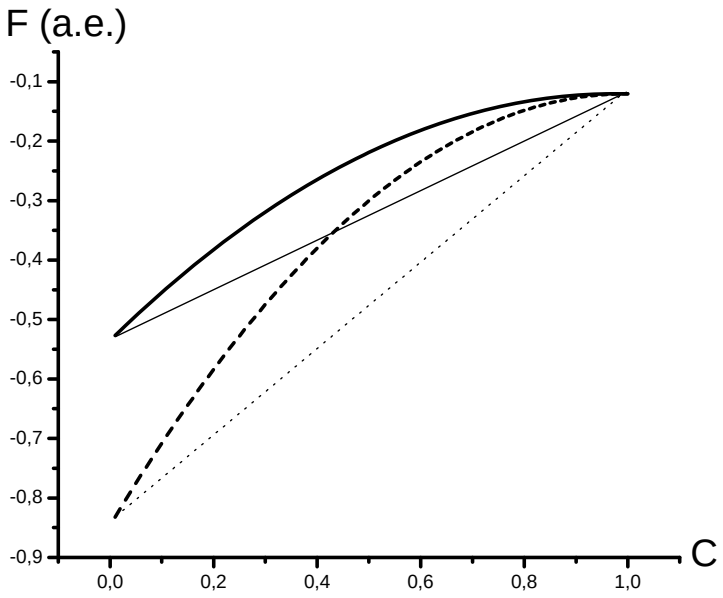

Fig.4.1.3. Dependence of thermodynamic potential of composite material vs concentration; solid line - for LaB_6-ZrB_2, and dotted one – LaB_6-TiB_2.

Energy of mixing

$$\Delta U = U_{AB} - \frac{1}{2}(U_{AA} + U_{BB}) \qquad (4.1.23)$$

defines type and measure of stability of this phase [64]. In case ΔU < 0 interaction of atoms of dissimilar components is stronger than that of atoms of same component (they form continuous number of solid solutions), and at ΔU > 0 there occurs a disintegration on two solid solutions of different concentration.

As indicator of formation of eutectic in solid phase the following condition is used [64]:

$$\Delta U > 2kT\,, \qquad (4.1.24)$$

where T - any temperature from the area of existence of given phase.

Alloys composition in system $A - B$, as well as temperature in eutectic point is defined from conditions

$$\frac{\partial F}{\partial C} = 0\ ; \qquad \frac{\partial F}{\partial T} = 0\,. \qquad (4.1.25)$$

Eventually we obtain a system from two algebraic equations with two unknowns - C_E (for component A) and T_E .

Results and discussions

Lattice parameters of elementary cells are defined on minimum of system's total energy. Calculated values of energy of interaction between components in investigated systems are presented in [65-66]. The results of calculations are available in tables 4.1.2-4.1.7. Calculated values of parameters of crystal lattices are in a good agreement with experimental data.

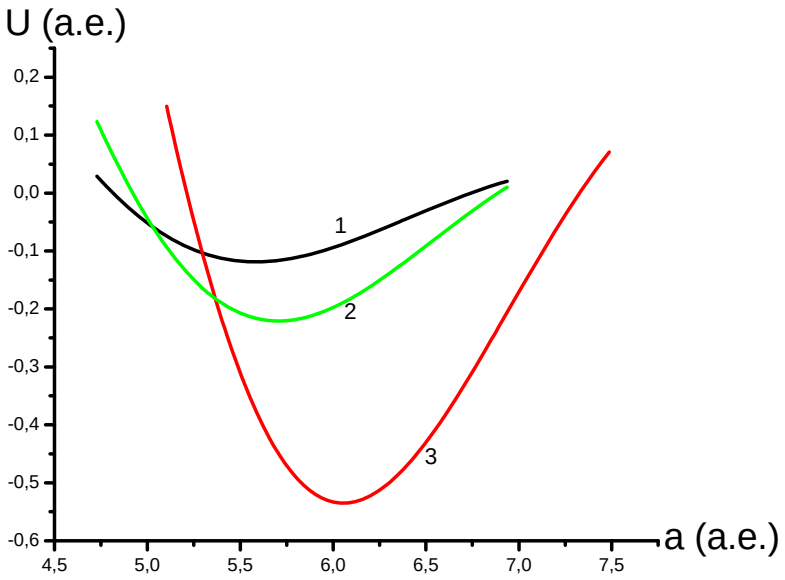

Fig.4.1.4. Dependence of energy of electron-ion system vs parameter of basic plane (1 – LaB_6; 2 – LaB_6 - ZrB_2 ; 3 - ZrB_2)

At calculation of energy of interaction of two components U_{AB} it is necessary to choose a boundary of joining of elementary cells and here we accounted for all possible configuration of cells joining. In system LaB_6 – MeB_2 possible joining is illustrated on figs. 4.1.5-4.1.6. We used those values of energy at which the system is stable (i.e. has a minimum energy).

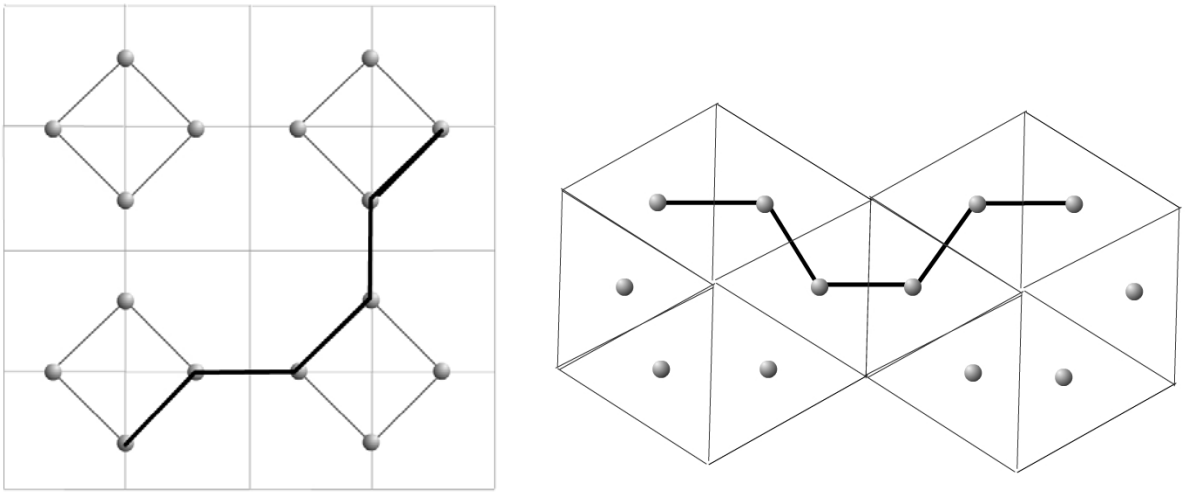

Fig.4.1.5. Location of boron atoms in plane [002] in elementary cell LaB_6 and MeB_2.

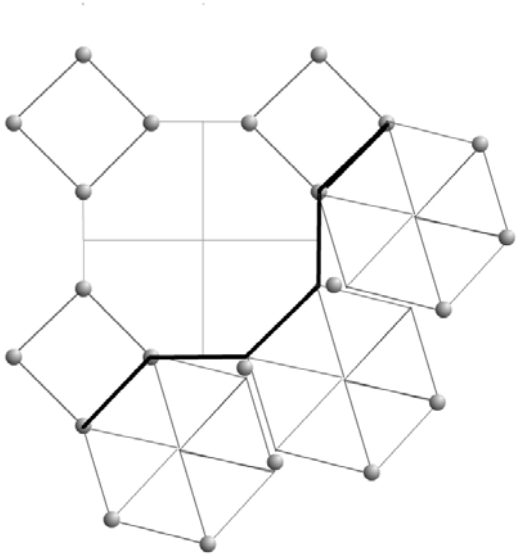

Fig.4.1.6 Joining of atomic planes [002] LaB_6 and MeB_2.

Table 4.1.2. Lattice parameters, internal energy for components and bulk composite material (as well as energy of mixing) for systems LaB_6-MeB_2 in atomic units ($\hbar = e = m = 1$), ω - oscillation frequency in units sec^{-1} (U_{11} - U_{AA} or U_{BB})

	a, c lattice parameters calculated experimental [57]	$-U_{mm}$	$-U_{AB}$ LaB_6- MeB_2	ω $\cdot 10^{13}$ sec^{-1}	ΔU
LaB_6	7,897 7,948	0,84145		0,04727	
TiB_2	5,709; 6,138; 5,709; 6,1377	2,18914	0,2233	0,0577	1,29199
ZrB_2	6,065; 6,59; 5,99; 6,673	1,6979	0,207618	0,04216	0,99928
HfB_2	5,985; 6,47; 5,936; 6,529	2,0934	0,2106	0,066236	1,2568

VB_2	5,642; 5,804; 5,67; 5,784	0,5429	0,2338	0,04334	0,45837
CrB_2	5,62; 5,779; 5,61; 5,783	0,53276	0,23482	0,041568	0,45228

Calculated values of energy of interaction between components in the investigated systems are presented in table 4.1.2. Lattice parameters of elementary cells are defined on minimum of total energy of system. Calculations were made for concentration $C_0 = 0;\ 0{,}5;\ 1$ of one of the component. In case $C_0 = 0{,}5$ all possible variants of joining of elementary cells of two different components were considered. Calculated values of lattice parameters of components differ only slightly.

For all investigated materials the energy of mixing ΔU [65-66] has:

1) positive sign that confirms experimentally defined fact about complete mutual insolubility of strengthening components in matrix;

2) $\Delta U > 2kT_{\max}$ ($T_{\max}$ - max temperature of given phase, i.e. melting temperature of refractory component), that is sufficient and required condition for eutectic formation in the investigated system.

For VB_2 ΔU - has min value if compare with other composite materials on the base of LaB_6 and diborides of transitive metals [3], $\Delta U = 0{,}225184 \cdot 10^{-18}$ Joule and $2kT_{\max} = 0{,}1656648 \cdot 10^{-18}$ Joule, i.e. the following condition is true $\Delta U > 2kT_{\max}$. Table 4.1.2 presents values ΔU and $2kT_{\max}$ for the rest of the investigated systems.

Concentration compositions and temperatures correspondent to eutectic ration are confirmed (table 4.1.3).

Table 4.1.3. Characteristics of eutectic composite materials in system LaB_6-MeB_2

MeB_2	c_E (calculated) %		c_E (experimental) %			T_E K^0	
	mol	volume	mol. [11]	volume	volume [1-5]	Calcul.	Exp [1-5]
TiB_2	25	10,497	34	16	10,7	2600	2680
ZrB_2	31,1	16,22	32	16	16,3	2750	2740
HfB_2	22,5	12,38	30	16	12,6	2770	2750
VB_2	54,2	29,10	69	38	29,6	2550	2580
CrB_2	61,9	41,34	73	48	45,2	2460	2470
NbB_2	39,3	19,77	43	23	20,2	2720	2710
TaB_2	28,5	12,98	40	21	13,1	2740	2730

By means of the method of pseudo-potential in the second order of perturbation theory for

composite alloys in systems LaB_6 MeB_2 we calculated:

- Parameters of crystal lattices, components and systems as a whole;
- Internal energy of components;
- Energy of interaction between molecules of components of composite alloys;
- Energy of interplane interaction for components;
- Energy of mixture, which for all investigated alloys satisfies the condition of formation of eutectic at temperature T (where T - temperature from an interval of existence of a solid phase);
- Frequencies of thermal fluctuations of molecules of these systems;
- Energy of thermal fluctuations of molecules in terms of Einstein's model.
- Concentration of components and values of temperatures in eutectic point;

Analysing the results of numerical experiment we may assert that the suggested model that uses pseudopotential rather good describes a behaviour and state of the investigated self-reinforced eutectic quasibinary alloys.

4.2 Structures design

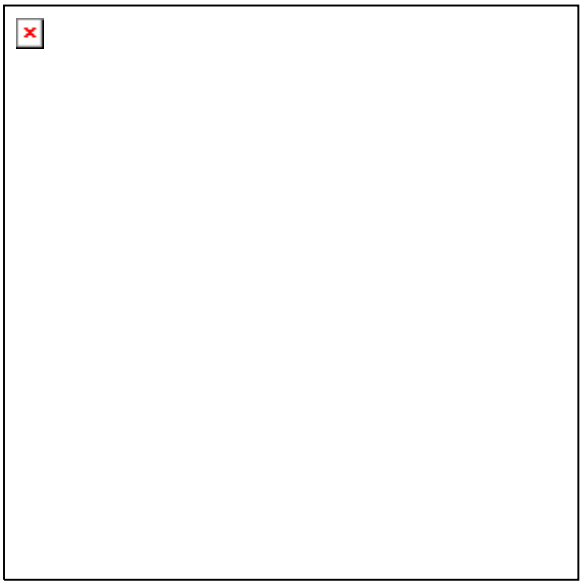

The primary goal of investigation in this direction is to design universal, geometrical-topological model of appearance, selection and evolution of cluster substructural units in nonequilibrium processes of crystals formation of given chemical compounds.

A common property of crystal solid bodies is global coherentness in a spatial arrangement of atoms. Mathematically, atoms are characterized by three-dimensional 3D lattices (or point lattices), being a geometrical image of group of T translations. It should be noted that any discrete structure including atomic crystal structure, mathematically could be presented as a graph, which tops – atoms, and bonds among those – graph edges [76].

All existing models of structure of crystal structures are geometrical-topological models *only describing* a global structure of atomic ensembles (discrete sets) in two extreme conditions: pre - – there is a "system - chaos" and post solidification – "system - crystal".

Up to now there has been no algorithmically developed model of transition from the ordered Delaney's systems to ordered systems, described by crystal lattices.

Usually (r_D, R) - Delaney's systems considered in the modern literature sources 1980-2007 [77-80] are static. These systems are shot of a parameter describing evolution atomic systems. This key parameter of a system is time [81]. In (r_D, R) - Delaney's systems a program of irreversible evolution of system at microlevel is absent – not highlighted the types of possible trajectories of change of atomic structure of clusters along «time row»; not considered the sequences of transitions from elementary to more complicated structures spontaneously appearing in system. The most important at the analysis of systems evolution is an introduction of the rules of selection of special types of isomers from a set of topologically possible, through definition of informational-significant clusters [81] and modeling on of an assembly of periodic structures with different dimension on the base of those clusters.

In terms of a physical model an algorithm (scenario) of evolutionary behavior of system should be determined. A direction of primary development of system and its possible change in time (after transition to higher level of self-organization) should be supervised by a change of values of some universal parameters of system, which are required to be precisely determined. Three-dimensional symmetry only reflects a specificity of structural interactions in system at all levels of self-organization and should be derived (obtained) at cluster modeling of an assembly of crystal structures (and not *visa versa*).

As self-organization we understand a phenomenon of spontaneous formation of ordered spatial *structures* in nonequilibrium open systems. To this type of systems we may refer crystal forming systems, in which there is a spontaneous appearance of long range ordering in arrangement of structural units (SU) of any nature (atoms, micro- and macromolecules, clusters), originally existing as a chaotic mixture; this process is called as crystallization.

In lab conditions, to obtain a single crystal compounds with given architecture and interesting physical and chemical properties, a labor-consuming search of appropriate conditions is required to initiate a crystallization, - i.e. selection of appropriate density of flows of chemical reagents and a variation of temperature and pressure. Hierarchical levels of complexity of organized matter growing in time in physics of structurally - organized condensed phases schematically can be presented as following sequence:

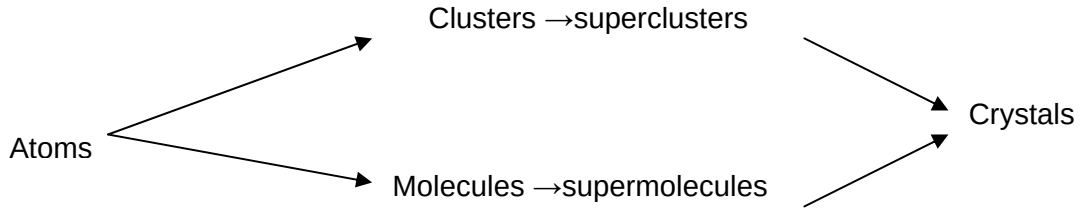

A distinction among molecules and clusters – only in nature of interpartical bonds (not covalent and covalent) at transition of system to higher level of self-organization and these distinctions come to light only during system evolution. In crystal forming system appearing as a result of its evolution, solid bodies have long range ordering – global structure or large-scale coherence in arrangement of particles of any

nature. For clusters in the majority of element compounds (formed less than 100 atoms in the Periodic system) all bonds among atoms at all levels of self-organization of system remain indiscernible and there occurs a formation of three-dimensional structures *of a frame type* with equal (or approximately equal) lengths of interatomic bonds. Thus a memory about cluster (island-like) nature *of predecessor of structure* in a macrocrystalline condition may appear not preserved. Special methods of combinatory-topological analysis for its revealing *in all* known *crystal structures* are required. Elementary compounds - elementary on structure and more difficult objects of inorganic nature - silicates and synthetic phases – high-temperature superconductors of layered cuprates [83, 84] are referred to those crystal structures. For the last it is revealed more than thirty structural types (the most complicated compounds on chemical composition), for the first time obtained during the last 15 years. For all crystal structures a presence of cluster level of formation of predecessors is postulated, and crystallization in system is considered as kinetic transition like "disorder - order" appearing under a certain program of matrix assembly. The problem of cluster self-organization in atomic systems elementary on structure from originally chaotic mixture of microatomic formations – clusters – stepped forth on a foreground at modeling of the processes of crystals growth only recently.

The most widespread structure on a boundary «melt-crystal (solid body)» is cubic I-structure (with bulk-centered Brave lattice). For this structure a value of coordination number (CN) is accepted as 14 (i.e. a sum of values 8+6) or only 8.

The analysis and explanation of known experimental data (on structure, composition of crystal phases and conditions of their reception) should be carried out in terms of algorithmically designed geometrical-topological model of formation, selection and evolution of clusters. Accordingly, a solution of a problem of modeling of processes of self-organization of atomic systems would be carried out through disclosing of mechanisms of intercluster condensation. Thus a cause-effect relation in a form of a program of assembly of structures would be wrote as significant sequences of elementary events resulting in occurrence of long range ordering and an arrangement of structural units. Actual problem of physics of condensed condition (and natural sciences as a whole) is modeling of processes of self-organization in nonequilibrium systems and in an end, an explanation of proceeding of the processes of self-organization at microscopic, cluster level, as complimentary, highly selective assembly of structures from microparticles with different chemical compound of atoms.

Let's accept the following crystallographic definition of cluster-predecessor and super predecessor of crystal structure.

Cluster-predecessor of structure is *a multiatomic cluster (from two and more atoms, determined as some monomeric subunit), condensation of cluster at all stages of assembly of structure occurs on the mechanism of complimentary bonding and is supervised by triple selection on transmitting symmetry*.

Super predecessor of structure is *overcluster structure of a high level (supercluster, superpredecessor), revealed as a result of algorithmically carried out modeling of the process of complimentary assembly of crystal structure from cluster-predecessor (monomeric subunit)*.

After identification of cluster-predecessor a common scheme of algorithm of assembly of any crystal structure of frame type looks as follows:

1 level: cluster-monometer $\rightarrow$ dimer (short circuit from monometers);

2 level: dimer (short circuit) $\rightarrow$ tetramer (layer from short circuits);

3 level: tetramer (layer from short circuits) $\rightarrow$ octamer (microframe from layers).

Hierarchical ratio between cluster-predecessor and superpredecessor of crystal structure are obvious. The first is an island-like 0-dimensional predecessor (pro-predecessor) of three-dimensional superpredecessor.

In structures with chain-like structure – the superpredecessor is defined on the first level of covalent self-organization of system (level of formation of repeating link of the chain), for phases with layered structure - at the second level of self-organization (formation of a layer from covalent-bonded chains).

The general scheme of matrix self-assembling of crystal structure has three partially overlapped stages of self-organization of systems accepted in physical models of kinetic transitions like "disorder - order":

- Small-scale fluctuations – "template" stage: formation and disintegration of the elementary associators from atomic clusters or molecules in system; minimal degree of complimentary bonding.
- Mesoscale fluctuations – "self-organization" of system: formation of more long-living (stable) cluster ensembles in a form of short chains, microlayers and microframes; in case of molecular systems – complimentary formation from molecules of two or three-dimensional associators as supramolecular ensembles.
- Large-scale fluctuations (phenomenon autocatalysis) – "self-assembly" of system: complimentary three-dimensional condensation of cluster *superpredecessors* or super (supra) molecular ensembles; a stage of formation of global crystal *structures*.

One of the principles of macrostructural evolution of inorganic systems implies a preservation of system *in integrated condition*, first of all, *crystal forming particles*, as particles with other things being equal most quickly reaching a high level of hierarchical self-organization.

Let's introduce and illustrate the basic geometrical conceptions, which we further would use at description of self-assembly of atomic systems:

Euclidean space usually designated as R^n is called n-dimensional vector space in which scalar product of vectors is determined.

Let's consider a discrete set of points $P = \{P_1 P_2, P_{3..}\}$ in space R^n. Then three following concepts [84] can be determined.

Radius of covering of point P_i, is usually designated as *R* and is the least upper boundary for a distance from any point from R^n up to the nearest point P_i. If this upper boundary does not exist, then $R = \infty$. Spheres of radius *R* with centers in points from P cover the whole space R^n.

Voronoy polyhedron V (P_i) The polyhedron is built around each point P_i. It consists of points of space R^n which are as close to P_i as to any other point Pj. *Voronoy polyhedrons* are also called as *Dirihle areas, Brillouin zones or Vigner -Zejts cells.*

Voronoy polyhedrons are not crossed, but they have general edges. Each edge lays in a plane, equidistant from two next points P_i. e *Voronoy polyhedrons* are convex polyhedrons. Association of

these polyhedrons coincides with the whole R^n. If a set P forms a lattice, then all *Voronoy polyhedrons* are congruent.

As an example let's consider a cluster from 19 atoms, represented on *fig. 4.2.1a.* Centers of atoms on fig. 4.2.1b are presented as a set of bonded points P_i. Topology of bonds of atoms in ensemble characterizes structural graph, where atoms (graph vertexes) are bonded by direct lines (graph edges). The coordination sequence for central atom in cluster looks like (6, 12). Built square matrix of connectivity of graph vertexes with dimension 19x19 would show a presence of three groups of vertexes with different local environment. Three and four bonds characterize on six vertexes on cluster boundary, six bonds have other seven graph vertexes. *Voronoy polyhedrons* of spherical packing — regular hexagon (fig. 4.2.1c).

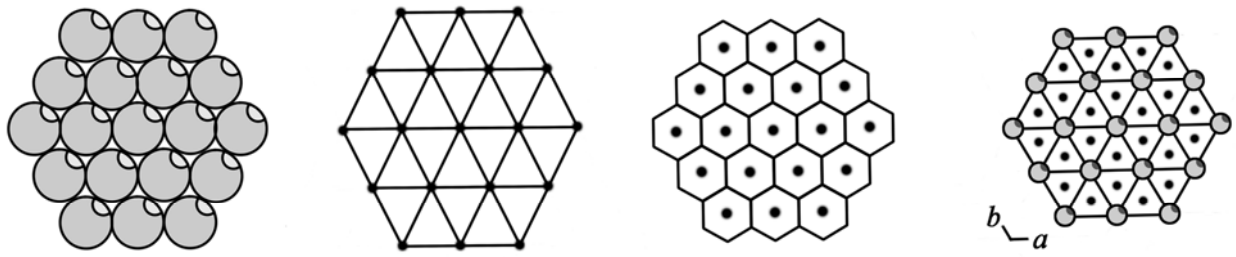

a) b) c) d)

Fig. 4.2.1 Bidimentional hexagon packing from rigid spheres: a) represented *as* spheres touching each other; b) representation as bonded points — graph vertexes; c) *Voronoy polyhedrons* — regular hexagons (center of polyhedrons — small balls) are allocated. *Voronoy polyhedrons* completely (intervals free) fill in a plane; d) Delone areas — triangles (center — "empty" black Delone sphere) are allocated. Delone areas from triangles completely fill in a plane

Delone area is defined for each vertex of *Voronoy polyhedron*; is a polyhedron being a convex environment of points from P, the nearest to given vertex.

Delone areas also form splitting of space R^n into convex parts. Such splitting is dual with regard to splitting of the space on *Voronoy polyhedrons*.

On a plane a physical sense of allocation of Delone areas in infinite atomic systems is in definition of types of locally bonded groups of atoms (clusters); a description of cyclic subgraphs (i.e. the system is characterized by certain set of n-polygons) is carried out. Delone areas with polyhedral structure (as a convex environment) are allocated in space of atomic system.

Fig. 4.2.1.d illustrates Delone areas for 19-atomic cluster. The areas look like triangles (the center of each triangle has "empty" black Delone sphere).

Delone areas from triangles as well as *Voronoy polyhedrons* (intervals free) fill in the plane.

Set of points of Eulerian spaces R^n is called as (r_D, R) Delone system if its points meet the following two requirements (axioms) [77-80]:

1. *Distance between any two points of the set is more than some fixed piece of length r_D.*

2. *Distance from any point of the space up to the point of a set nearest to it is less than some fixed piece of length R.*

In point (geometrical) models of description of atomic systems a relationship of r_D and R is analyzed. In physical models for the characteristic of atoms of system let's in addition introduce a value of radius of atom *r.*

The first axiom, as applied to real atomic systems, implies a fact that the centers of atoms in any atomic formation can not approach as much as close to each other owing to final sizes of atoms. Accordingly, the minimum value of Delone sphere put into between centres of atoms, can be equal only $r_D = 2r$.

At modeling of atomic clusters the value *2r* we accept as minimum possible atomic distance S (A-A) for atoms A which form cluster. Other values of interatomic distances S (A-A) at increase of a number of contacts among atoms may be equal 2r or more *2r, for example,* at formation of not covalent bonds by two-atomic molecules.

The second axiom implies the universal nature of condensed condition of real physical system (gas, liquid, solid body). In system it is possible an introduction of final distance among particles so that radiuses *L* described around all particles, would completely cover the whole space and that among those a special final radius, with value $L = L_{max}$ would be equal *R.*

There exist ultimate values of particles density and if they are reached there is a formation of crystal structures and, *visa versa*, if particles density falls up to some minimal value crystallization is terminated. It is associated with strengthening (fracture) of spatial-time correlations in process of increase of particles density in system. In more dense environments particles have no time to fall apart up to the elementary components and as clusters participate further in intercluster interactions.

In terms of the general theory of systems two introduced axioms mean, that:

a) objects of system (considered as discrete (indivisible) particles - atoms with radius *r* are determined*;*

b) local characteristics of pair interactions of atoms in atomic ensemble (final minimal value r_D and final maximal distance between atoms in system which correlates with value *R)* are set*.*

Imposing of the third (additional) condition on a relative positioning of centers of atoms (points) in space, namely [78, 80]:

c) each of points in system possesses equality of a local milieu of other points, results in systems of points which meet to a distant arrangement of centers of atoms in crystal structures (crystal *lattices*).

The last condition defines a final macrocondition of evolutioning atomic system.

In real physical structures atoms in lattices are overlapped, as they are not absolutely rigid – occurs overlapping of external electron envelopes of spheres - atoms. In models of structures of importance is to

calculate a special case of an arrangement of spheres in lattices of different dimension when the volume of overlapped areas of spheres would be minimal (most economic) In three-dimensional space this property is referred to cubic I-lattice [84].

At crystallization local symmetry of cluster is not that important but a mechanism of construction of a chain – layer – a frame and preservation of transmitting periodicity at all stages of assembly.

The theory of graphs is an area of finite mathematics studying discrete structures, named as graphs. In crystallography the theory of graphs is applied to modeling of classification and investigation of combinatory-topological properties of topological clusters.

In common view – *graph* is set of points (vertexes) and a set of pairs of these points (not necessary all), bonded by lines (edges).

Other basic concepts of the theory of graphs which are used in further work:

Way in graph – alternating sequence of vertexes in which any of vertexes does not repeat.

Contour – closed way in which the first and the last vertexes coincide.

Chain of graph – sequence of edges in which any of vertexes does not repeat.

Cycle – closed chain in which its initial and final vertexes coincide.

Graph is called as bound if any pair of its vertexes is bonded by a chain and/or way; otherwise graphs are called as *inconsistent*.

For solution of topological problems the graphs are represented by means of *adjacency matrixes* in which lines and columns meet numbers of graph vertexes. Elements accept values 0 and 1 (that accordingly characterizes the absence and presence of bond between given pair of vertexes with chosen numbers). Diagonal elements of the matrix are zero by definition.

The theory of graphs and regular polyhedrons is an auxiliary mathematical apparatus, which does not enter into a circle of interests of materials science teams (and consequently general educational courses) however is required for understanding of suggested ways of solution put before us in this investigation.

Let's get back to designing of clusters. Definition of bonded atom – atom in a molecule (cluster) should enable a possibility to define all its properties. Due to physical continuity this definition should turn to quantum-mechanical definition of appropriate properties of isolated atom.

Two identical samples of substance possess identical properties. This simple fact may be distributed on atoms and to demand, that atoms are to determined in real space in a way that for identical atoms in two different systems or in different parts of one system (for example, in a solid body) a contribution of this atom to complete properties of system is identical. Atoms – objects in real space. A theory defines those atoms through a division of real space, basing on topological properties of molecular distribution of electronic density (ED), i.e. its kind in a real space. A constancy of properties of atom in theory, including its contribution to complete energy of system, should be directly defined by an appropriate constancy of its ED distribution. If ED distribution in two different molecules are the same, i.e. in a real space of two systems the atom or some functional group of atoms are identical, they provide an identical contribution into complete energy and other properties in both systems. It falls from a direct relationship between a spatial form of atom and its properties, which we may identify in different systems.

In definition of topological properties of molecular distribution ED a nucleus plays an important role, being so-called ***attractor,*** which may be used for definition of atom. At this approach a chemical individuality of atom is defined by ED distribution. A question «if there are atoms in molecules (clusters)? » is an equivalent to two equally obvious questions of quantum mechanics: whether a state function ψ(**x**, t), containing an information about a system may predict unique division of a molecule into subsystems and if yes, whether it is possible to define observable values as well as their average values and equations of motion for subsystems? Affirmative answers to these both questions are required for description of physics of atom in a molecule or cluster by means of quantum mechanics. One should account for, that quantum subsystems are open systems determined in a real space, and their boundaries are defined by specific properties ED. The state function ψ defines the information, which may be known about a quantum system. In a theory of molecular structure, free from any or subjective assumptions, any information apart from that one involved in ψ should not be used. State function for molecular system is a function of electronic and atomic coordinates and time ψ **(x, X,** t**),** where **x -** spatial and spin coordinates of electrons, **X -** sets of nuclear coordinates, t **-** time.

Electronic density ρ **(r)** is a fundamental characteristic measured in experiment on coherent dispersion of X-rays, which usually is carried out at definition of crystal structure. Namely from intensity of diffused x-ray radiation it is possible to obtain structural amplitudes, and their Fourier-transformation gives electronic density ρ **(r)**. Distribution ED in a point **r** of elementary cell is described by equation

$$\rho(\vec{r}) = V^{-1}\sum_{h}\sum_{k}\sum_{l} F(hkl)\exp(-2\pi ip\cdot\kappa) \qquad (4.2.1)$$

where V – volume of elementary cell, $F(hkl)$ - structural amplitude

$$F(hkl) = \sum_{J} f_J \exp\left(2\pi i\vec{h}\cdot\vec{r}_J\right), \qquad (4.2.2)$$

where f_J - atomic amplitude of dissipation of j atom in elementary cell and $\mathbf{r}_j$ - its position. Components of vector **h** look like ***h/****a,* ***k/****b,* and ***l/****c*, where a, b and c – sizes of edges of elementary cell. It is experimentally found, that maxima meet positions of atomic nucleus and consequently, formula (4.2.1) may be used for definition of an arrangement of atoms in a crystal. Thus, a mathematical description of crystal structure brings to Fourier series, which represents a distribution of electronic density. Methods of overcoming of collateral problems appearing at such description (like thermal degradation of nucleus positions) are constantly improved and equality (4.2.1) finds a wide application for ρ **(r)** definition of the results of X-ray experiment on dispersion [86-89]. Stuart [90] derived a ratio, which allow to design maps of electro-statistic properties EP (and also a vector field of a gradient and Laplacian density associated with it) directly from experimentally found x-ray structures of amplitudes.

The electronic density ρ ***(r)*** is a physical value with some value in each point of space and representing a scalar field, defined in 3D space. Topological properties of this field are usually considered in terms of a number and type of its critical points. These points in which the first derivatives ρ ***(r)*** are zero, define positions of extrema ED (maxima, minima or saddle values). As ED is not arbitrary field, but the field, which kind is defined by forces acting on electronic density on the part of nucleus, its topological structure is a rather simple. This structure becomes more obvious and more easy is subjected to an

analysis while investigation of the vector of a gradient of electronic density associated with a field $\nabla\rho$ **(r).** The image $\nabla\rho$ **(r)** for a concrete molecule enables without any further mathematical analysis to visualize its atoms and some sets of lines connecting certain pairs of nucleus in a molecule – its molecular graph. Almost all molecular models (a model of spherical atom suggested by Bragg for modeling of crystal structures, more modern model of overlapped Van der Waals spheres and models of filling of spaces usually used by chemists for definition of molecules form and size) reflect a fact that ED has a maximum on a nucleus and falls down almost spherically at moving off this point. Even for not so complicated molecule ED may have maxima (and in fact, special points) in separately chosen plane and, hence, knowledge ρ (**r**) in one or two measurements it is not enough to characterize its form in 3D space. In conjunction with that a general method of exact description of basic topological features of distribution ED is required. This information is provided with values of curvature ρ (**r**) in its critical points [69, 76].

Values of curvature in a critical point ρ can be found (as latent vectors and appropriate proper values) by diagonalization of Hessian matrix ρ ($\mathbf{r}_c$). Thus, a terms «curvature and proper value » and «axes of curvature and latent vectors » can be used as synonyms at description of properties of critical point ED. All proper values of Hessian matrix ρ in a critical point are real and can be also equal to zero. *A rank* of critical point designated ω is equal to a number of nonzero proper values (i.e. values of curvature ρ*)* in critical point. The attribute σ is simple algebraic sum of signs of proper values, i.e. signs of values of curvature ρ in critical point (let's call it as attribute of a sign in a critical point or *a signature).* The critical point is characterized by these two sizes *(ω, σ).* Therefore, for example, a central critical point in ethylene with three nonzero values of curvature (one positive and two negative) is a critical point of type (3,—1).

Behind a rather rare exception all critical points of distributions ED of molecules at energetically stable geometrical configurations of nucleus or near vicinities of those have a rank equal three. A fact of this prevalence of critical points with ω = 3 — general observation associated with features of topology of distribution ED in molecules. In terms of properties of critical points with ω = 3 elements of molecular structure are defined. A critical point with ω <3, i.e. at least with one zero curvature is called as degenerated. Such critical point is instable in a sense that a small change of ED caused by displacement of nucleus, results in its disappearance or bifurcation on a number of non-degenerate or stable *(ω* = 3) critical points. As a structure is characteristic in a sense that it (as it is or as a set of bonds) is kept in a certain range of configurations of nucleus, an observable rarity of non-degenerate critical points is not surprising. One may expect, that appearance of degenerated critical point ED of a molecule means the beginning of structural change. There are only four possible values of attribute σ at critical points of the third rank:

(3,-3) All values of curvature are negative and ρ has a local maximum in $\mathbf{r_c}$.

(3,-1) Two values of curvature are negative and ρ has a maximum in $\mathbf{r}_c$ in a plane determined by corresponding axes. Along the third axis, perpendicular this plane, ρ has a minimum in $\mathbf{r_c}$.

(3, +1) Two values of curvature are positive and ρ has a minimum in $\mathbf{r}_c$ in a plane determined by corresponding axes. Along the third axis, perpendicular this plane, in a point $\mathbf{r_c}$ ρ has a maximum.

(3, +3) All values of curvature are positive and ρ has a local minimum in a point $\mathbf{r_c}$.

ED involves structural information, which is determining for the field of a vector of gradient associated with that. We noticed that unique local maxima in distribution of density of multi-electronic system meet positions of nucleus. This supervision provides a nucleus with a special role as attractor (points of attraction) in a field of vector of gradient ED. This identification (it reflects a main role of nuclear forces in definition of ρ) makes a basis for definition of atom and other elements of molecular structure. Besides it would be interesting on the basis of the analysis of vector field ED to express through its parameters the boundary conditions for a quantum subsystem. Thus, a vector field of gradient ED may be used both for quantum definition of subsystems, and for cartography of elements of cluster structure (that may enable to build a theory of atoms in clusters, considered as uniting structures).

The vector field of gradient ED may be presented by an image of a trajectory, made by vector ∇ρ. A trajectory ∇ρ, called also as gradient line, begins in some arbitrary point $\mathbf{r}_0$ and is obtained by calculation ∇ρ $\mathbf{(r_0)}$ at displacement on distance Δ**r** from this point in a direction, which specifies the vector ∇ρ ($\mathbf{r}_0$). Procedure repeats until a line obtained in this way comes to an end.

1. As the vector of gradient of scalar value specifies a direction of its biggest increase, the trajectories ∇ρ are perpendicular to lines of constant density - contour lines ρ.
2. Vector ∇ρ **(r)** is directed on a tangent to a trajectory in each point **r**.
3. Each trajectory should begin and/or come to an end in a point, where ∇ρ **(r)** is equal to zero, i.e. in a critical point ρ.
4. Trajectories cannot be crossed, as ∇ρ **(r)** defines only one direction in each point **r**.

The critical point of type (3,—3) describes a property point attractor of a vector field of gradient ED: there is an open vicinity of attractor B, which is invariant to a flow ∇ρ so any trajectory starting in B, comes to an end in a point of attractor. The biggest vicinity satisfying these conditions is called as a pool of attractor.

As critical points of type (3,-3) in multi-electron distribution ED meet mainly only the positions of nucleus, the last operate as attractors of field of a vector of gradient ρ ***(r,*** **X**). Thereof, a real space of molecular distribution ED can be divided into not crossed areas — pools, each of which contains one point either attractor or a nucleus. Free or bonded atom is defined as association of attractor and a pool associated with it.

At the same time the atom can be determined in terms of its boundaries. A pool of individual nuclear attractor in isolated atom covers full 3D space R^3. For atom in cluster the nuclear pool is open subset R^3. It is separated from the pools of neibouring atoms by interatomic surfaces. The existence of interatomic surface S_{AB} means a presence of critical point of type (3,-1) between the neibouring nucleus A and B.

The presence of critical point of type (3,-1) and the line of atomic interaction associated with it specify that ED is accumulated between nucleuses bonding those. In this point the line of atomic interaction crosses interatomic surface and electrons thus are collected between nucleuses along this line. Both the theory and the observable facts confirm that accumulation of ED between pair of nucleuses is a required condition of bonding of one atom with another. The same condition becomes sufficient when inter-nucleus forces are balanced and the system is characterized by geometry with minimum equilibrium energy. Thus, the presence of a line of atomic interaction in this equilibrium geometry satisfies both

required and sufficient conditions of bonding of atoms with each other. The line of maximum ED bonding nucleuses is called *as communication line,* a critical point of type (3,—1) — *a critical point of communication* [93].

For given nuclear configuration X *molecular graph* is defined as closed set of lines or lines of atomic interaction. Molecular graph is represented by a set of communication lines of connecting pairs of neibouring nuclear attractors. This graph allocates pair interactions presented in ensemble of atoms which mainly characterize system properties as well as conditions of its balance or change.

Molecular graph here is a direct consequence of the main topological properties of ED distribution of system: local maxima — critical points of type (3,-3) — are observed in positions of nucleus, defining atoms, and critical points of type (3,-1) bond (but not all) pairs of nucleus in cluster. Set of the communication lines obtained thus as appeared, coincides with a set of bonded pairs of atoms, which may be suggested on the basis of chemical reasons. To representation of chemical structure as the set of communication lines one managed to come by generalization of data about combination of chemical elements and models of their bonding. In particular, it concerns a model of chemical valency, which asserts that ability of given type of atom to formation of bonds (valency) can be saturated and be defined by a number of valent electrons. For definition of any chemical structure it is necessary to have a lot of data about it and accordingly the same information successfully and briefly is expressed by these structures. Demonstration that molecular structure can be precisely presented by molecular graph provides with new information, namely, that nucleuses formally united by valent strokes in structure are turned to be incorporated in space by communication lines along which there occurs a maximum accumulation of electronic density which by itself represents an original chemical "glue".

A number and type of critical points, which can coexist in system with final number of nucleus are obeyed to Puankare - Hopf ratio. In view of the mentioned interrelation between type of critical point and element of molecular structure, this ratio is formulated as follows:

$$n - b + r - c = 1 \qquad (4.2.3)$$

where: n — number of nucleuses, b — number of communication lines (or lines of atomic interaction), r — number of cycles, and c — number of cells [91]. A set of numbers *(n,b,r,c)* is *characteristic* for each cluster.

Being based on above said and involving preliminary results obtained by our colleagues – crystallographers (who have yet to consider these complicated systems, but for more simple systems have interesting results) in a solution of a problem of cluster designing of ceramic composites of system LaB_6-MeB_2 (and systems close to it) we are about to move this way. All clusters are formed from a base package of clusters, which contains (2 dimensions) - regular polygons (3D) -regular (or Archimedean) polyhedrons. Thus each cluster has a "solid" nucleus and a "soft" jacket.

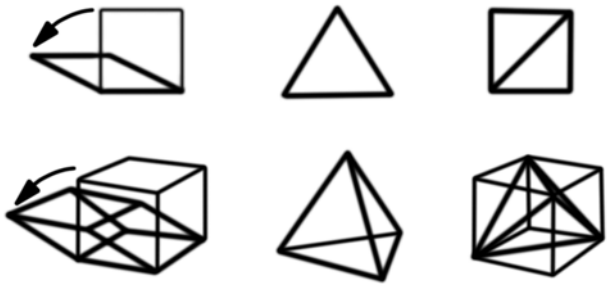

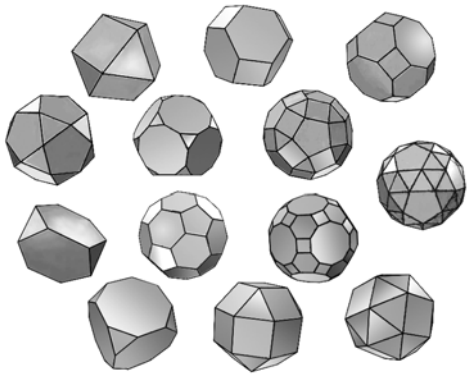

Base clusters are bonded with chemical composition of "islands" in a bouillon of melt, which crystallizes. This bouillon involves both separate atoms (monomers) and linear formations (dimers). **The first problem** is to learn how to build it base clusters for real substances and especially for those systems, which are of our interest: LaB_6-MeB_2 etc.

At once let's define **what is what**? The center of cluster – is its center of mass. Lengths of sides are associated with interatomic distances. The solid nucleus "is associated" with ionic skeleton, and a soft jacket with valent electrons. What is this relationship let's formulate proceeding from the rules of this game in which we are going to play. Meanwhile we see two games. The first is «make a carpet » and the second - «solidify a bouillon». Moreover it is necessary to remember, that corners both in base clusters and in mosaics are bonded by valent angles.

Essence of the game «make a carpet»: Let's build N_1, N_2, N_3, …..N_m base clusters proceeding from concentration of chemical elements and kinds of their stable compounds (alloy state diagram).

Further, combining base clusters by selection let's stick together those on sides of identical length (with a tolerance for a soft jacket) in a mosaic carpet filling a plane (space). It is necessary to think over the rules of sticking but it is another (special) problem. We also have to think over a number of checks of viability of formed clusters on each step of building (physics and chemistry). At the certain rules this "carpet" may have holes (porosity).

Essence of the game «solidify a bouillon»: let's have a tank with set law of heat removal where we have atoms, diners, clusters given by certain distribution associated with concentration of components. Initial temperature T_0 sets a distribution of speeds of participants of events. We set rules of interaction of

bouillon elements at impact (when they stick together, when they have an elastic impact, etc.) and we include a heat removal as well. Clusters start to grow and to slow down. Gel solidifies and forms (single crystal, polycrystal, amorphous body, quasicrystal...) and all this depending on the rules which we set. Here too should be a set of checks (physics, chemistry), which will exclude impractical exotic. Here is a field of work for molecular dynamics of mesoparticles. Fortunately we always know the center of mass of current cluster and its characteristics.

In this game it is possible to implement a transition of amorphous body in crystal. Most likely, it is a bouillon with rather high concentration of clusters with rather big sizes.

This game first of all should clarify an initial stage of crystallization process: *monomers* → *dimmer* → *cluster* and further (through interaction of clusters) → consolidated substance (amorphous body, quasicrystal, crystal, etc.).

Problems: 1. Computer design: a) regular polygons with jackets of set thickness; b) regular (and Archimedean) polyhedrons with jackets of set thickness.

2. to build (a) plane, b) volumetric) lattices of investigated systems LaB_6-MeB_2 and to allocate variants of base clusters with well defined torn off bonds in those.

3. to develop variants of rules of (a) sticking b) impacts of base clusters, being based on physical and chemical properties of these processes (molecular dynamics and chemical reactions)

4. to develop potentials of interaction among clusters – mesoparticles built in item 2.

5. to pick up variants of molecular dynamics for realization of the game «solidify a bouillon».

Solution of these problems at the moment of contract accomplishment is an intermediate state, which as we believe, should not be discussed as of yet. The obtained results will be employed for further work and would be accounted by means of shortening of time for appropriate stages in working schedule of the next contract.

5. Conclusions

Macroscale

1. The simplest model of directed solidification process for boride composites MeB_6-MeB_2 based on sample's mass and energy conservation laws brings to a conclusion that in the mode of low crystallization rates 0,5 mm/min < v < 4 mm/min diameter of fiber of reinforcing component MeB_2 increases with a growth of crystallization rate, that points out a difference in crystallization mechanisms for the investigated materials depending on ultimate value (v ~ 5 mm/min) of pulling rate.

2. Equations of steady-state diffusion describe fields of concentration of materials of matrix and reinforcing phase in melt up to crystallization front with rather good accuracy.

3. Crystallization occurs in a very narrow zone close to crystallization front and its width essentially decreases with a growth of pulling rate.

4. Apparatus to resolve a problem of heat transfer with moving boundary caused by change of substance aggregate state, that further would enable to apply it for solution of definite problems realizing the technology of directed solidification for eutectic systems LaB_6-MeB_2 has been developed.

5. Asymptotic method of Bahvalov-Sanches-Palensia enabled to calculate elastic constants and fields of thermo-deformation for both real eutectic systems LaB_6-MeB_2 and hypothetic nanocomposites of these systems with different volume share of nanotubular reinforcing whiskers. For macrocomposites the results obtained are in a good agreement with experimental ones, and for nanocomposites the predicted characteristics are very attractive, that makes a problem of modification of DSEC technology actual for nanotubular whiskers.

Mesoscale

1. The methodology of definition of multifractal characteristics of materials structure has been prepared on the base of analysis of images obtained by SPM.

2. A number of compulsory requirements for preparation of a package of analyzed images to elevate the adequacy of definition of structure dependent properties of the investigated composites has been developed.

Microscale

1. Being based on quantum-mechanical approach (the method of a priori pseudopotential), values of temperature and concentration of components in eutectic point for the system LaB_6-MeB_2 were for the first time, theoretically obtained. The results obtained are in a good agreement with experimental data.

2. Apparatus and algorithm of cluster designing of bimonocrystals in systems LaB_6-MeB_2 have been developed. Realization of this algorithm requires rather a big volume of further additional investigations.

6. Closing

The results submitted in this report have two scientifically important components. The first is – fragments of accomplished parts of investigations targeted on realization of project's objective. They were reflected both in the report and open Russian and English periodicals [65-66], [85-99]. The second component is – the groundwork, which may serve a solid background for further investigation. They are based on the analysis of existing publications (mainly those concerning other more simple systems) the experience gained in discussions with specialists from allied fields of knowledge and a very big volume of numerical testing experiment. Summary of this component is very schematic and leaves in a shadow (and in many cases failures) difficulties of adaptation of the existing models of more simple systems for the investigated system LaB_6-MeB_2 and testing of the suggested models. A big problem was also to obtain reliable experimental data required for numerical experiments. However all these questions during the contract performance have been regularly discussed Dr. Ali Sayir, scientific coordinator of this project, and they always have (as a result of these discussions) constructiveness defining both further direction of research activity of this project and formulation of content and volume of those problems, which would be enclosed in the follow-up projects.

Project team hope that these final report would be interesting and useful for colleagues involved in DSEC issues and properties of composites obtained by directed solidification.

7. References

1. Odarian S.S., Paderno Yu.B., Nikolaeva I.I., Horoshilova E.K. Interaction in system LaB_6 – ZrB_2 // Powder metallurgy. – 1983. - №11. – pp. 87-90.
2. Paderno Yu., Paderno V., Filipov V. Some peculiarities of structure formation in eutectic d- and f-transition metals boride alloys // Boron-rich solids, AIF Conf. proc. N 231. — Albuquerque: NM, 1990. — P. 561—569.
3. Odarian S.S., Paderno Yu.B., Nikolaeva I.I., Horoshilova E.K. Interaction in system LaB_6 – TiB_2 // Inorganic materials – 1984. – T. 20, № 5. – pp. 850-851.
4. Odarian S.S., Paderno Yu.B., Nikolaeva I.I., Horoshilova E.K. Interaction in system LaB_6 – HfB_2 // Powder metallurgy. – 1984. - № 2 . – pp. 79- 81.
5. Odarian S.S., Paderno Yu.B., Nikolaeva I.I., Horoshilova E.K. Interaction in system LaB_6 – CrB_2 // Powder metallurgy. – 1984. - № 5. – pp. 66- 68.
6. Paderno Yuri, Paderno Varvara, Filipov Vladimir, Some Crystal Chemistry relationships in eutectic co-crystallization of d- and f-transition metal borides // J. Alloys and Compounds.- 1995, **219,** P.116-118.
7. Paderno Yu.B., Paderno V., Filipov V. Some peculiarities Crystallization of LaB_6-(Ti, Zr)B_2 Alloys // J. Solid State Chemistry.-2000, **154,** P.165-167.
8. Paderno Yu.B. A new class of “in-situ” fiber reinforced boride composite ceramic materials // in “Advanced Multilayered and Fibre-Reinforced Composites” (Y.M.Haddad, Ed), Kluwer Academic, Dordrecht.-1998, P.353-369.
9. Chen Chang-Ming, Zhou Wang-Cheng, Zhang Li-Tong, Oriented Structure and Crystallography of directionally Solidified LaB_6-ZrB_2 Eutectic // J. Am. Ceram. Soc.- 1998, **81,** № 1, P.237-240.
10. Chen Chang-Ming, Zhang L.T., Zhou W.C. Characterization of LaB_6-ZrB_2 eutectic composite growth by the floating zone method // J. Crystal Growth.- 1998, **191**, P.873-878.
11. Odarian S.S. «About regularities of interaction in system LaB_6 – Me $^{IV-VI}$ B_2 // inorganic materials series. -1988 –T24. –№2.- pp. 235-238.
12. Samsonov G.V. Refractory compounds. Handbook on properties and application M., 1963.
13. Physics of solid body. Thesaurus. Kyiv. Naukova dumka. 1996. T.1. – pp.651.
14. Frantsevich E.N., Voronov F.F., Bakuta S.A. Elastic constants and modulus of elasticity of metals and nonmetals Reference book. Kyiv. Naukova dumka. 1982.- pp.286.
15. Elbaum K. –Success of Physical Science, 1963, 79, 3, 545
16. Tiller W. A. The Art and Science of the Growing Crystals. Ed. J.J. Gilman, London, N.Y., 1963, 276.
17. Kyropulos S.-Zs. Anorg. U.allg. Chem., 1925, 154. 308.
18. Czochralski J.-Zs. Phys. Chem., 1918. 92. 219.
19. Stockbarger D.-Rev. Sci. Iustr., 1936, 7,133.
20. Stober F/-Zc. Krist., 1925, 61, 299.
21. Stepanov E.V., Vasilieva M.A.- in book: Crystals growth, 3 Publishing house AN USSR, M., 1961, 223-238.
22. Bolling G.F.A. Tiller W.A.-J. Appl. Phys. 1960, 31, 1345.

23. Lubov B.Ja. Roytburd A.L., Temkin D.I. – in book: Crystals growth, 3 Publishing house AN USSR, M., 1961, 68-74.
24. Stefan F.-Monatass. Math.u. Phys., 1890,1, 1/
25. Borisov V.T., Любов Б.Я., Temkin D.I. –DAN USSR, 1955, 104, 2, 223.
26. Lubov B.Ja., Temkin D.I. – in book: Problems of materials science and physics of metals. Metallurgizdat, M., 1958, 311-316.
27. Temkin D.I.– Engineering and Physical Journal, 1962, 4, 89-92.
28. Birman B.E. – in book: Crystals growth, 5 Publishing house AN USSR, 1965.
29. Ivantsov G.P. – DAN USSR, 1947, 58, 567.
30. Horvey G.a. Cahn J.W. – Acta met., 1962, 9, 695-705.
31. Paderno Yu.B., Paderno V.N., Filipov V.B. Derected solidified ceramic fibrous-strengthened boride composites // Ogneupori and technical ceramics. 2000. №11.ppC.2-7.
32. Tiller W. A. Liquid Metals and Solidification. – Cleveland: ASM, 1958. – 276 p.
33. Chalmers B. Principles of Solidification. – New York-London-Sydney: John Wiley & Sons Inc, 1964. – 288 p.
34. Budak B.M., Goldman N.L., Egorova A.T., Uspenskiy A.B. method of fronts straightening for solution fo Stephan's problem in multidimensional case //Numerical methods and programming. M.:MGU, 1967. – vol. 8. – pp. 103-120.
35. Budak B.M., Solovieva I.N., Uspenskiy A.B. Difference method with smoothening of coefficients for solution of Stephan's problem // Journal of numerical mathematics and mathematical physics. – 1965. – vol.5, № 5. – pp. 828-840.
36. Vabishevich P.N. Numerical methods for solution of problems with free boundary. – M.: Publishing house of Moscow university, 1987. – p. 164
37. Meymanov A.M. Stephan's problem. Novosibirsk. Nauka Siberian Department AN USSR, 1986. – p. 239.
38. Gerebiatiev E.F., Lukianov A.T. Mathematical modeling of processes of heat- and mass transfer with moving boundaries. Alma Ata: Gilim, 1992. – p. 264.
39. Olshanski V.Yu. Mathematical modeling of process of thermo-expansion of graphite with account for phase transitions // IX All Union Meeting on theoretical and applied mechanics. Proceedings N.-Novgorod, August 23-28, 2006: N. Novgorod, 2006.
40. Rubinshteyn L.E. Stephan's problem Riga: Zvayzgne, 1967. –p. 457
41. Samarskiy A.A., Vabishev P.N. Additive schemes for problems of mathematical physics. – M.: Nauka, 2001. – p. 319
42. Samarskiy A.A., Moiseenko B.D. Economic scheme of end-to-end calculation of multidimensional Stephan's problem // Journal of numerical mathematics and mathematical physics. – 1965. – vol.5, № 5. – pp. 816-827.
43. Belonosov S.M. Application of theory of potentials to one-dimensional Stephan's problem. In book: Applied numerical analysis and mathematical modeling. Vladivostok: Far Pacific Area AN USSR, 1980

44. E. Sanches-Palencia Non-Homogeneons Media and Vibration Theory Springer-Verglag New York 1980.
45. N.S. Bashvalov, G.P. Panasenko. Averaging of processes in periodic environments. Moscow. Nauka 1984. in Russian
46. Andrievski R.A. Nanomaterials: conception and modern problems //Russian chemical journal –2002. vol.46, №5, pp.50-66
47. Andrievski R.A., Glezer A.M. Size effects in nanocrystalline materials II. Mechanical and Physical properties //Physics of metal and materials science 2000. vol 89, №1, pp.91-112.
48. Mandelbrot B.B. *The Fractal Geometry of Nature.* — San Francisco: W.H.Freeman, 1982.
49. Feder J. *Fractals*. New York: Plenum Press, 1988.
50. Jaffard S. *Multifractal Formalism for Functions*. — Philadelphia: SIAM, 1997.
51. Kartuzov V.V., Trefilov V.I., Minakov N.V. Fractal dimension of break surfaces. — Physical metallurgy and thermal treatment of metals. 2001. — №3. — pp.10-14.
52. Vstovsky G.V. Found.Phys. 1997, v.27, №10, p.1413-1444.
53. Pande C.S., Richards L.E., Louat N. et al.// Acta Metall. Mater. 1987. V.35. №7. P.1633.
54. Almqvist N.// Surf. Sci. 1996. V.355. P.221.
55. Orme C., Johnson M.D., Leung K.T., Orr B.G. // Mater. Sci. Eng. B. 1995. V.30. №2-3, P.143.
56. Somov A.I., Tihonovsky M.A. Eutectic compositions. - M.: Metallurgy, 1975.- p.305.
57. Samsonov G. V., Serebriakova T. I., Neronov V. A. Borides. – M.: Atomizdat, 1975. – p. 375.
58. Heyne V., Koen M., Uer D. Pseudopotential theory. – M.: Mir, 1973.
59. Pilenkevich A.N., Zakarian D.A. Model non-local pseudopotential. 1. Simple metals // SPJ.- 1985.-**30**, №12. – C.1861-1865.; Model non-local pseudopotential. 2. Diamond and $BN_{c\Phi}$ // ibid -1986.- **31**, № 1.- pp. 93-96.; Model non-local pseudopotential. 3. Transitive metals// ibid - 1986**.- 31**, №4 .- pp.609-615.
60. Zayman J. Principles of theory of solid state. – M.: Mir, 1966.
61. Kitel Ch. Introduction in physics of solid body. –M.: Nauka, 1976.
62. Zakarian D.A., Kartuzov V.V. Calculation of theoretical strength of diamond-like materials, falling from energy of interaction of atomic planes// Reports of NANU – 2006. - №7. – pp. 94-99.
63. Landau L.D., Lifshits I.M. Statistical physics. M.: Nauka, 1976.
64. Shultz G. Physics of metals. – M.: Mir, 1971.- p.503.
65. Zakarian D.A., Kartuzov V.V., Hachatrian A. V. On the base of pseudopotential method design of thermodynamic potentials of eutectic alloys LaB_6 –MeB_2 (Me- Ti, Zr) **//** Works of IPMS NANU Mathematical modeling and numerical experiment in materials science Kyiv – 2007.- 9**. – pp**. 8-12.
66. Zakarian D.A., Kartuzov V.V., Hachatrian A. V. Calculation of typical parameters of alloys LaB_6 –MeB_2 being based on pseudopotential method **//** Works of IPMS NANU Mathematical modeling and numerical experiment in materials science Kyiv – 2008.- 10**. –** c.21-27.

67. Wells A.F. Three – dimensional nets and polyhedra New York: Interscience, 1977. 263 p.
68. Galiulin R.V. Geometrical theory of crystals formation// Crystallography 1998. vol.43, №2, pp. 366-374 .
69. Galiulin R.V. Crystallographic geometry. M. Nauka, 1984, p.135
70. Galiulin R.V. Delone's systems // Crystallography. 1980. vol.5. p. 901-908
71. Galiulin R.V. Crystallographic picture of the world //SPS. 2002. vol.772, №2, pp.229-233.
72. Ilyushin G.D. Demianets L.N., Crystal structure formation of silicates in accordance with the mechanism of matrix assembly //19 European Crystallographic Meeting, Nancy, 2000, 25-31 August P.362
73. Ilyushin G.D. Demianets L.N.,. General principles of construction of metal-oxide superconductors //Superconductivity. 1990, vol.3, №12, pp. 1908-1915
74. Ilyushin G.D. Demianets L.N., Structural aspect of high temperature superconductors //VI conference of crystal-chemistry of inorganic and coordination compounds. Lviv, 1992. p. 143
75. Convey J. Sloen N. Packaging of balls, lettice and group. Vol. 1,2. M. Mir, 1990, p. 415
76. Engel P. Geometries Crystallography. Dordrecht: D /Reidel Publishing Company, 1986 /266p.
77. Kalkhan M., Tsirelson V.G., Ozerov R.P. DAN USSR , 303, 404 (1988).
78. Tsirelson V.G., Ozerov R.P. Electron Density and Bonding in Crystals. Institute of Physics Publ.: Bristol and Philadelphia, 1996.
79. Tsirelson V.G. Chemical bond and heat movement of atoms in crystals. -M: VINITI, 1993. – p.262
80. Tsirelson V.G., Can. J. Chem., 74, 1171-1179 (1997)
81. Stewart R.F. Chem. Phys. Lett. 65, 335 (1979).
82. Collard K., Hall G.G. Int.J. Quantum Chem, 12, 623 (1977).
83. Smith V.H., Price P.F. Absar I. Israel J.Chem . 16, 187 (1977).
84. Bader R.F. W., Essen H.J. Chem. Phys., 80, 1943 (1984).
85. E.I. Krasikova, I.V. Krasikov, V.V. Kartuzov. Definition of fractal characteristics of materials structure by the method of multifractal analysis of images. Numerical experiment on model objects. Mathematical models and numerical experiment in materials science. Works of IPMS NASU. -2007, vol. 9. - pp. 79 – 84.
86. Baranovskaja L.V. Some test examples for numerical realization of functional-differential problems of materials science // Mathematical models and numerical experiment in materials science. Works of IPMS NASU. -2008, vol. 10. pp. 72-77.
87. E.I. Krasikova, I.V. Krasikov, V.V. Kartuzov. About stability of definition of multifractural characteristics of nanostructures using electron microscopy images. V International inter discipline symposium FIPS-08 "Applied synergetic in nanotechnologies" November 17-20, Moscow, 2008.
88. Kartuzov V.V., Baranovskaja L.V. Stephan's problem as a model of non-stationary mode of directed solidification of composites LaB_6-MeB_2 (Me-Ti, Zr, Hf)// Materials of VII scientific conference named after academician M. Kravchuk, Kyiv, 2008, p.174.

89. Kartuzov V.V., Baranovskaja L.V. Functional-differential equations of self-organized systems with memory// V International inter discipline symposium FIPS-08 “Applied synergetic in nanotechnologies” November 17-20, Moscow, 2008, pp.112-115.
90. Zakarian D.A,, Kartuzov V.V, Hachatrian A.V. Calculation of thermodynamic potentials for systems B_4C – TiB_2 , TiB_2 - SiC, B_4C - SiC by means of pseudopotential //Powder metallurgy 2009. - № 9-10 . – pp.124-132.
91. Zakarian D.A,, Kartuzov V.V, Hachatrian A.V. Definition of typical parameters (temperature, concentration) of eutectic in system Hf – HfB by means of pseudopotential method // Mathematical models and numerical experiment in materials science. Works of IPMS NASU Kyiv, Ukraine -2009, vol. 11. - pp.3 - 9.
92. Zakarian D.A,, Kartuzov V.V, Hachatrian A.V. MakaraV.A., Hachatrian A.V. Computer modelling of conditions of eutectic formation in system Hf – HfB (NANU Reports, in press).
93. Zakarian D.A,, Kartuzov V.V, Kartuzov E.V., Hachatrian A.V. Calculation of composition in LaB_6-ZrB_2 and LaB_6-ZrB_2 eutectics by means of pseudopotential method // Jour. Of the European Ceramic Society (in press).
94. Zakarian D.A., Kartuzov V.V, Kartuzov E.V., Hachatrian A.V., A.Sayir. Pseudopotential method of calculation of temperature and concentration of eutectics invariant point LAB6 - MeB2 (Me - Ti, Zr, V, Cr, Hf)// Phys Rev (in press).
95. B. A. Galanov, E. A. Iefimova, V. B. Filipov, V. V. Kartuzov, T. V. Kartuzov, V.N. Paderno, A.Sayr. Modelling of Structure Formation of Ceramic Fiber Boride Composites at Directed Solidification of Eutectic Alloys // Jour. Of the European Ceramic Society (in press).
96. Zakarian D.A., Kartuzov V.V., Kartuzov E.V. Hachatrian A.V. Calculation of composition in LaB_6-ZrB_2 and LaB_6-ZrB_2 eutectics by means of pseudopotential method. Workshop on Aerospace Materials Extreme Environments, held in St. Louis, Missouri, USA, August 3-5, 2009.
97. B. A. Galanov, E. A. Iefimova, V. B. Filipov, V. V. Kartuzov, Y. V. Kartuzov, V.N. Paderno. Modelling of Structure Formation of Ceramic Fiber Boride Composites at Directed Solidification of Eutectic Alloys. Workshop on Aerospace Materials Extreme Environments, held in St. Louis, Missouri, USA, August 3-5, 2009.
98. E. Kartuzov, B.Galanov, E.Efimova, V.Kartuzov. Steady-state diffusion in binary eutectic mixture LaB_6-MeB_2 (Me-Zr, Ti) at direction solidification from melt. 3rd Directionally Solidified Eutectic Ceramics Workshop, November 10-13, 2009 - Seville, Spain.
99. E. Kartuzov, D. Zakarian, A. Hachatrian, V. Kartuzov. "Steady-state diffusion in binary eutectic mixture LaB_6-MeB_2 (Me-Zr, Ti) at directed solidification from melt" на 3rd Directionally Solidified Eutectic Ceramics Workshop, November 10-13, 2009 - Seville, Spain.